



This is to certify that the

thesis entitled

KINETICS OF DESORPTION OF BOVINE SERUM ALBUMIN AT THE OIL-WATER INTERFACE USING TOTAL INTERNAL REFLECTION FLUORESCENCE AND FLUORESCENCE PHOTOBLEACHING RECOVERY

presented by

Brian Shukla

has been accepted towards fulfillment of the requirements for

M.S. degree in Chemical Engineering

Date 8/17/98

MSU is an Affirmative Action/Equal Opportunity Institution

0-7639



PLACE IN RETURN BOX to remove this checkout from your record. TO AVOID FINES return on or before date due.

DATE DUE	DATE DUE	DATE DUE

1/98 c:/CIRC/DateDue.p65-p.14

KINETICS OF DESORPTION OF BOVINE SERUM ALBUMIN AT THE OIL-WATER INTERFACE USING TOTAL INTERNAL REFLECTION FLUORESCENCE AND FLUORESCENCE PHOTOBLEACHING RECOVERY

By

Brian Shukla

A THESIS

Submitted to
Michigan State University
in partial fulfillment of the requirements
for the degree of

MASTER OF SCIENCE

Department of Chemical Engineering

1998

ABSTRACT

KINETICS OF DESORPTION OF BOVINE SERUM ALBUMIN AT THE OIL-WATER INTERFACE USING TOTAL INTERNAL REFLECTION FLUORESCENCE AND FLUORESCENCE PHOTOBLEACHING RECOVERY

By

Brian Shukla

The primary objective of this thesis was to measure the kinetics of desorption of bovine serum albumin (BSA) labeled with fluorescein-5-isothiocyanate (FITC) at the oil-water interface. We used a 5-W argon ion laser, an inverted microscope, and a photomultiplier tube connected to a data acquisition system. We measured the dynamics of protein desorption by total internal reflection fluorescence (TIRF) microscopy, along with fluorescence photobleaching recovery (FPR).

Fluorescence recovery data were fit to a biexponential kinetic model to extract the rate constants. At a bulk BSA-FITC concentration of 0.07 mM (millimoles per liter), the apparent fast desorption rate constant (k_1) was 0.52 ± 0.12 s⁻¹, the apparent slow desorption rate constant (k_2) had a value of 0.008 ± 0.003 s⁻¹, and the immobile fraction (r_0) was calculated as 0.46 ± 0.04 . Slow photobleaching effects were accounted for by introducing a slow photobleaching rate constant (k_{pb}) into the analytical model. We demonstrated that failure to account for slow photobleaching effects leads to an overestimation of the immobile fraction. A low signal to noise ratio contributed to some uncertainty in the desorption rate constants.



ACKNOWLEDGMENTS

I would like to thank my advisor, Dr. Robert Y. Ofoli, for guiding and encouraging me during the course of my studies and research. Thanks also to Ari Gajraj, Jamaica Prince, and Sumei Wei for providing helpful input on my project, with additional thanks to Ari for working diligently with me to get the equipment ready for experimentation. I would also like to thank Parijat Jauhari, whose thesis work showed that TIRF could be used to study protein interactions at the oil-water interface. Finally, I would like to thank the Department of Chemical Engineering at Michigan State University for giving me this opportunity to further my intellectual growth.

TABLE OF CONTENTS

LIST OF FIGURES	vi
LIST OF TABLES	viii
1. INTRODUCTION	1
1.1 Motivation for this study	1
1.2 Objectives	
2. THEORY	
2.1 TIR excitation at a single interface	
2.2 Fluorescence Photobleaching Recovery (FPR)	
2.3 Adsorption/desorption kinetics at an interface	6
3. EXPERIMENTAL MATERIALS AND TECHNIQUES	11
3.1 Materials preparation	
3.1.1 Technique for protein labeling	
3.1.2 PEO coating of bottom slide	
3.2 Experimental equipment	
3.2.1 TIRF/FPR setup	
3.2.2 The experimental cell	
3.3 Experimental techniques	
3.3.1 The oil-water interface	
3.3.2 Focusing of microscope objective at the liquid-liquid interface	
3.3.3 Fluorescence photobleaching recovery (FPR)	
4. ANALYSIS TECHNIQUE	
4.1 A biexponential trend in the kinetics of desorption	
4.2 Accounting for slow photobleaching due to the monitoring beam	
4.3 Analysis of TIRF/FPR data	27
5. RESULTS AND DISCUSSION	29
5.1 Desorption kinetics of BSA-FITC at an oil-water interface	
5.2 Discussion	
5.3 Possible sources of error	
6. SUMMARY AND CONCLUSIONS	54
7. SUGGESTIONS FOR FUTURE WORK	57
7.1 Protein adsorption onto a clean interface	57
7.2 Effect of labeling ratio on protein desorption kinetics	
8 RIRI IOCD ADHV	61

LIST OF FIGURES

Figure 2.1: Total internal reflection, with resulting evanescent wave, at an oil-water interface. The evanescent wave decays exponentially into the rarer medium
Figure 3.1: TIRF/FPR equipment. The laser beam is first split into photobleaching and monitoring beams and then recombined by optical flats before being directed to the oil-water interface. The PMT is used to collect the fluorescence emission
Figure 3.2: The experimental cell, or "flowcell." Note that the top view shows an "open" cell, meaning that the prism and top slide have been removed to give an internal view of the cell.
Figure 3.3: TIRF/FPR experiment showing one effect of improper focusing of the microscope objective. A photobleaching pulse occurs at time 15 seconds, but no post-bleaching drop in intensity is observed, because the microscope objective is focused in the bulk protein solution, rather than at the oil-water interface
Figure 5.1: Typical fluorescence recovery curve for TIRF/FPR experiments. Initially, there is a fast recovery of fluorescence (1), which is followed by a slower period of recovery (2). The fluorescence does not completely recover to its pre-bleach level (3), indicating that a fraction of photobleached proteins are irreversibly adsorbed to the interface. $F(-)$ is the equilibrium fluorescence prior to photobleaching, and $F(0)$ is the fluorescence immediately after the photobleaching flash, which occurs approximately 10 seconds into the experiment and has a duration of 100 ms. The bulk protein concentration for this data was 0.04 mM
Figure 5.2: Drop in fluorescence during a long experiment, due to slow photobleaching by the monitoring beam. The fluorescence level abruptly drops after the photobleaching flash. A partial recovery of fluorescence occurs over a brief period (1), after which the fluorescence level slowly drops, due to unintended photobleaching (2). The bulk protein concentration for this data was 0.04 mM
Figure 5.3: Apparent rapid desorption rate constant k_1 as a function of bulk protein concentration. Each data point represents the average of twenty experiments conducted at room temperature ($\sim 20^{\circ}$ C) and in the dark. The photobleaching pulse duration was 100 ms.
Figure 5.4: Apparent slow desorption rate constant k_2 as a function of bulk protein concentration. Each data point represents the average of twenty experiments conducted at room temperature ($\sim 20^{\circ}$ C) and in the dark. The photobleaching pulse duration was 100 ms.

Figure 5.5: Slow photobleaching rate constant k_{pb} as a function of bulk protein concentration. Each data point represents the average of twenty experiments conducted at room temperature (\sim 20°C) and in the dark. The photobleaching pulse duration was 100 ms.
Figure 5.6: Immobile fraction r_0 as a function of bulk protein concentration. Each data point represents the average of twenty experiments conducted at room temperature and in the dark. The photobleaching pulse duration was 100 ms
Figure 5.7: Fraction of proteins (r_1) that desorb at an apparent rate of k_1 , as a function of bulk protein concentration. Each data point represents the average of twenty experiments conducted at room temperature ($\sim 20^{\circ}$ C) and in the dark. The photobleaching pulse duration was 100 ms.
Figure 5.8: Fraction of proteins (r_2) that are more tightly held at the interface and desorb at an apparent rate of k_2 as a function of bulk protein concentration. Each data point represents the average of twenty experiments conducted at room temperature (~20°C) and in the dark. The photobleaching pulse duration was 100 ms
Figure 5.9: Short-term theoretical recovery curves generated from Eqn. [19], using the kinetic parameters obtained via curve fitting. The bulk concentration is 0.07 mM. The curve that assumes absence of slow photobleaching was generated by setting k_{pb} equal to zero in Eqn. [19]
Figure 5.10: Long-term theoretical recovery curves generated from Eqn. [19], using the kinetic parameters obtained via curve fitting. The bulk concentration is 0.07 mM The curve that assumes absence of slow photobleaching was generated by setting k_{pb} equal to zero in Eqn. [19]

LIST OF TABLES

Table 5.1: Summary of the apparent desorption and photobleaching rate constant	
BSA-FITC at the oil-water interface	33
Table 5.2: Values obtained for the immobile fraction (r_0) , and the fractions of protein	ns that
desorb at rates k_1 and k_2 (r_1 and r_2 , respectively)	34

1. INTRODUCTION

1.1 Motivation for this study

The ability to quantify the dynamic behavior of proteins at the liquid-liquid interface is of considerable industrial importance. The food processing industry uses proteins as emulsifiers to lower the interfacial tension between two immiscible liquid phases and facilitate the dispersion of one phase in the other (Dickinson *et al.* 1990). The stability of emulsions such as margarine and mayonnaise depends on the adsorption of proteins at the oil-water interface. The pharmaceutical industry needs to understand the behavior of drugs at biomembranes to determine their pharmacological activity. Biomembranes are structurally complex, but immiscible oil-water interfaces may be used as a simplified model in drug delivery experiments (Arai *et al.* 1996).

Total internal reflection fluorescence (TIRF) has been used extensively to quantify protein behavior at the solid-liquid and membrane-liquid interfaces (Axelrod 1981; Burghardt and Axelrod 1981; Thompson et al. 1981; Zimmerman et al. 1990; Hellen and Axelrod 1991; Pearce et al. 1992; Pisarchick et al. 1992). TIRF is ideal for molecular-level studies of the interfacial behavior of amphiphiles, because the fluorescence of molecules at and/or near the interface are detected preferentially to that of molecules in the bulk liquid. This is due to the nature of the evanescent wave formed by total internal reflection at the interface, as will be discussed in detail in Chapter 2.

TIRF, along with fluorescence photobleaching recovery (FPR), was recently used successfully in our laboratory to quantify the diffusion of proteins at and near an immiscible oil-water interface (Jauhari 1997). Jauhari's work has provided a framework upon which the present TIRF study is based, to study other aspects of protein dynamics at the liquid-liquid interface. This study focuses on the kinetics of protein desorption at the oil-water interface.

1.2 Objectives

The goal of this study is to measure the kinetics of desorption of bovine serum albumin (BSA) labeled with fluorescein-5-isothiocyanate (FITC) at the oil-water interface, using a combination of TIRF and FPR. The first part of the work involves the adjustment of the experimental TIRF apparatus to bring the system closer to the reaction limited regime (and thus further from the transport limited regime). It has been shown in previous studies (Thompson *et al.* 1981; Pearce *et al.* 1992; Pisarchick *et al.* 1992) that the system approaches the reaction limited regime as the depth of observed fluorescence decreases and as the bulk protein concentration increases.

The depth of the observed fluorescence is a function of several factors that are all constants in our experimental apparatus (please see Chapter 2), and therefore the fluorescence penetration depth is not readily adjustable. However, the system can be brought closer to the reaction limited regime by determining the optimum BSA-FITC concentration range for desorption studies. An effective method of determining whether

the system is reaction limited or not is to measure the fluorescence recovery as a function of bulk protein concentration. If the kinetics show little or no dependence on concentration, then the system is not limited by transport (diffusional) processes but rather by the rates of adsorption/desorption at the interface (Pearce et al. 1992; Pisarchick et al. 1992).

The second part of the work was to determine the apparent fast and slow desorption rate constants (k_1 and k_2 , respectively, as outlined later in this thesis) for BSA-FITC complexes at the oil-water interface. Optical perturbation, in the form of spot photobleaching, was used to move the system away from equilibrium. This was accomplished by flashing an intense beam of light briefly at the oil-water interface, causing an irreversible bleaching of labeled proteins at and near the interface. The resulting exchange between bleached and unbleached proteins at the interface is then monitored. The fluorescence recovery data as a function of time can be used, as described in Chapter 2, to determine the kinetics of desorption at the interface.

2. THEORY

2.1 TIR excitation at a single interface

When a beam of light passes through an optically transparent medium with a higher refractive index (n_1) and arrives at the interface between that medium and one of a lower refractive index (n_2) , it will undergo total internal reflection (TIR) if its angle of incidence θ , measured normal to the interface, exceeds a critical angle θ_c given by

$$\theta_c = \sin^{-1}\left(\frac{n_2}{n_1}\right)$$
 [1]

where $n_2 < n_1$.

Although TIR occurs for $\theta > \theta_c$, some energy penetrates the interface in the form of an evanescent wave (or electromagnetic field), as shown in Figure 2.1. The intensity of the evanescent wave, which is a function of depth below the interface, is given by

$$I(z) = I_0 \exp\left(-\frac{z}{d}\right)$$
 [2]

where I(z) is the intensity of light at depth z below the interface, I_0 is the intensity at the interface (z = 0), and d, the evanescent wave penetration depth, is given by

$$d = \frac{\lambda_0}{4\pi n_1 \sqrt{\sin^2 \theta - (n_2/n_1)^2}}$$
 [3]

where λ_0 is the wavelength of the incident light in a vacuum.

For our system, d has a fixed value of 144 nm.

A detailed analysis of the evanescent wave, in which the electric and magnetic components are treated in three spatial directions, is given by Axelrod, et al. (1992).

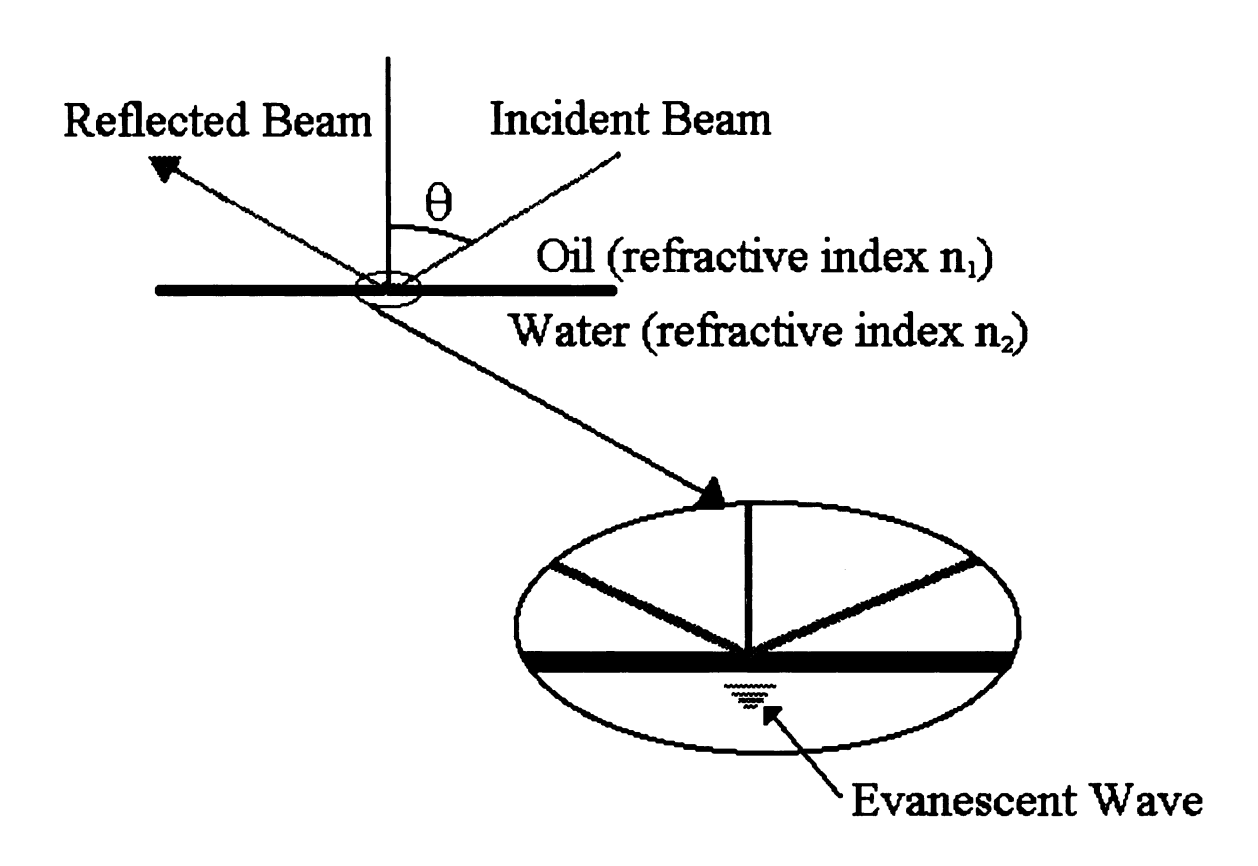


Figure 2.1: Total internal reflection, with resulting evanescent wave, at an oil-water interface. The evanescent wave decays exponentially into the rarer medium.

2.2 Fluorescence Photobleaching Recovery (FPR)

FPR is used to perturb the system and move it away from equilibrium. Fluorescence is induced in BSA-FITC molecules at and near the interface via an evanescent wave produced by a low intensity beam that we will refer to as the monitoring beam. A high intensity beam, called the photobleaching beam, is briefly flashed at the interface, photobleaching every fluorescent species within the field of the evanescent wave. When a fluorescent molecule is photobleached, it permanently loses its ability to fluoresce, due to a photochemical destruction of the fluorophore. Since the protein absorbs only small amounts of energy at the laser wavelength (488 nm) used for photobleaching, the fluorescent label is destroyed but not the protein. Once photobleaching has occurred, the fluorescence signal measured by the photomultiplier tube (PMT) will partially recover towards its prebleach level, due to the exchange of unbleached molecules in the bulk water phase with photobleached molecules at and very near the interface.

In this study, fluorescence photobleaching recovery has been used to characterize the kinetics of protein desorption at the oil-water interface. The fluorescence recovery profile following photobleaching was used to obtain desorption rate constants for the system.

2.3 Adsorption/desorption kinetics at an interface

Consider labeled amphiphilic molecules of bulk concentration [A] in equilibrium between an interface-bound state and a free solute state. The molecules can adsorb to free binding sites of interface concentration [B] to form complexes of interface concentration [C], or

the molecules can desorb from the complexes back into the bulk solution. This process can be represented as a chemical reaction of the form

$$A(r,z,t) + B(r,t) \xrightarrow{k_a \atop k_d} C(r,t)$$
 [4]

where k_a and k_d are the adsorption and desorption rate constants, respectively, r is the radial distance from the interface observation area to another point on the interface, z is the perpendicular distance from the interface observation area to a point in the bulk, and t is time.

In this context, binding refers to the adsorption of a molecule from the bulk solution onto an available site (or location) on the interface. The equilibrium of the system is described by

$$\frac{\overline{C}}{\overline{A}\overline{B}} = \frac{k_a}{k_d}$$
 [5]

where \overline{A} , \overline{B} , and \overline{C} are the equilibrium concentrations (bleached and unbleached) of A, B, and C, respectively.

Thompson et al. (1981) derived a mathematical model for use with TIRF/FPR experiments. A condensed version of their derivation is given below.

The differential equations governing A(r, z, t) and C(r, t) are, respectively

$$\frac{\partial A}{\partial t} = D_A \nabla_{r,z}^2 A \tag{6}$$

and

$$\frac{\partial C}{\partial t} = D_C \nabla_r^2 C + k_a A_{z \to 0} B - k_d C$$
 [7]

where D_A and D_C are the bulk and interface diffusion coefficients, respectively, ∇_r^2 and $\nabla_{r,z}^2$ are two and three dimensional Laplacian operators, respectively, and $A_{r\to 0} \equiv \lim_{r\to 0} A(r,z,t)$.

The task now is to relate fluorescence intensity to the interfacial concentration of proteins.

Thompson et al. (1981) showed that, following photobleaching

$$F(-) - F(t) = QI_0 \int \psi(r) (\overline{C} - C(r, t)) d^2r$$
 [8]

where F(-) is the equilibrium fluorescence prior to photobleaching, F(t) is the fluorescence at any time after the photobleaching flash (which occurs at t=0 by definition), Q is a product of the efficiencies of excitation light absorption and fluorescence emission and detection and is usually referred to as the quantum yield, I_0 is the maximum evanescent intensity at the interface, and $\psi(r)$ is a dimensionless evanescent intensity profile function with a maximum value of one.

After integrating Eqn. [8] and incorporating the initial and boundary conditions, Thompson et al. (1981) used linear transformation theory to obtain the following analytical solution:

$$F(-) - F(t) = \frac{F(-) - F(0)}{v_{-}^{1/2} - v_{+}^{1/2}} \left[v_{-}^{1/2} w \left(-i \sqrt{v_{+} k_{d} t} \right) - v_{+}^{1/2} w \left(-i \sqrt{v_{-} k_{d} t} \right) \right]$$
[9]

where

 $v_{\pm}^{1/2} = \frac{1}{2} \sqrt{\frac{k_d}{R_{BND}}} \left(-1 \pm \sqrt{1 - 4R_{BND} / k_d} \right)$ [10]

$$w(i\eta) = e^{\eta^2} \operatorname{erfc}(\eta) \qquad (\eta \text{ complex})$$
 [11]

and

$$R_{BND} \equiv \frac{D_A}{(\overline{C}/\overline{A})^2}$$
 (the "bulk normal diffusion rate") [12]

Equation [9] is impractical to use with experimental data, not only because of its complexity, but because it contains both bulk diffusional and desorption effects which will not be readily distinguishable in a TIRF/FPR experiment. However, if the desorption rate k_d is much smaller than the bulk normal diffusion rate R_{BND} , then the system will be in the reaction limited regime, and the functional dependence of Eqn. [9] on the bulk diffusion coefficient, D_A , will be negligible.

It has been shown in previous studies (Thompson et al. 1981; Pearce et al. 1992; Pisarchick et al. 1992) that increasing the bulk protein concentration brings the system closer to the reaction limited regime. Burghardt and Axelrod (1981) showed that, for bulk concentrations of BSA greater than or equal to 0.015 mM (millimoles per liter), fluorescence recovery is controlled by desorption reaction kinetics rather than by bulk diffusion. Under such conditions, Eqn. [9] reduces to the approximate form (Thompson et al. 1981)

$$F(-) - F(t) \approx [F(-) - F(0)]e^{-k_d t}$$
 [13]

Equation [13] represents the general form of the mathematical model used to analyze the TIRF/FPR data in this study. However, further modifications were made to this equation

to make it more appropriate for this work. These modifications are discussed in Chapter 4.

3. EXPERIMENTAL MATERIALS AND TECHNIQUES

3.1 Materials preparation

3.1.1 Technique for protein labeling

Bovine serum albumin (BSA), essentially fatty acid-free (A-7511, molecular weight ~67,000 g/mol), was obtained from the Sigma Chemical Co. (St. Louis, MO) and labeled with fluorescein-5-isothiocyanate (F-1907, molecular weight 389 g/mol, Molecular Probes, Eugene, OR) to form a BSA-FITC complex. FITC was covalently bonded to the lysine groups of BSA. All labeling reactions were done in a 0.10 M borax buffer (B-9876, Sigma Chemical Co., St. Louis, MO) for four hours at room temperature and pH ~9.2 in the dark, following the procedure described by Lok *et al.* (1983a).

To separate unconjugated FITC from BSA-FITC, the protein solution was dialyzed with stirring against a 0.03 M phosphate-buffered saline (PBS) buffer for 24 hours at pH ~7.4, using molecularporous regenerated cellulose dialysis membrane (Spectra/Por 1, molecular weight cutoff = 6,000, The Spectrum Companies, Gardena, CA). The solution was then dialyzed a second time for 24 hours using a second PBS buffer solution to further remove unconjugated FITC. During the dialysis process, PBS buffer exchanges with borax buffer, so that the protein solution within the dialysis bag is mostly PBS, and the pH is close to 7.4 as desired for the experiments conducted in this study. All buffers were made with deionized water from the NANOpure ultrapure water system (Barnstead, Dubuque, IA).

The labeling ratio of the protein, which is defined as the molar ratio of conjugated FITC to BSA, was determined spectrophotometrically using absorbance measurements at 280 nm for BSA and 488 nm for FITC. We used labeling ratios low enough to avoid concentration quenching, a phenomenon whose causes and effects were discussed in detail by Robeson (1995).

3.1.2 PEO coating of bottom slide

In order to prevent adsorption of protein molecules on the bottom interface of the experimental cell, the bottom slide (i.e. the bottom of the flowcell) was coated with poly(ethylene oxide) (PEO) (Cheng et al. 1987). Deionized water was used to make a 0.5 wt% PEO solution. A bottom glass slide, which had previously been cleaned using the procedure described by Cheng et al. (1987), was immersed in the PEO solution for two hours, thereby forming a PEO coating on the slide. Before the slide was used, it was rinsed with water to remove any excess PEO.

3.2 Experimental equipment

3.2.1 TIRF/FPR setup

The experimental setup used in our lab for TIRF/FPR experiments consists of a 5-W Lexel Model 95 continuous wave argon ion laser (Lexel Lasers, Inc., Fremont, CA), an Axiovert 135M inverted microscope (Carl Zeiss, Inc., Thornwood, NY), a photomultiplier tube (model R4632, Hamamatsu Corporation, Bridgewater, NJ) jacketed in a thermoelectric

cooling system (TE177TSRF, Products for Research, Inc., Danvers, MA) to increase the signal-to-noise ratio, a CCD camera (MTI, VE1000, Carl Zeiss, Inc., Thornwood, NY), a modular automation controller (MAC 2000, Ludl Electronic Products Ltd., Hawthorne, NY) with a computerized data acquisition system (Viewdac, Keithley Instruments, Inc., Rochester, NY), and a double-syringe pump (Model 551382, Harvard Apparatus, South Natick, MA). The entire setup sits on a vibration isolation table (RS 4000, Newport Corporation, Irvine, CA), which dampens vibrations from external sources, to mitigate against excessive mobility of the oil-water interface.

The laser, which operates at a wavelength of 488 nm, is attenuated using neutral density filters (03FNQ, Melles Griot, Boulder, CO). The original beam is first split into two beams (a monitoring beam and a photobleaching beam) of vastly unequal intensities, using an optical flat, and then recombined using a second optical flat. This arrangement ensures that the monitoring and photobleaching beams are perfectly aligned after recombination (Thomas and Webb 1990). In between the optical flats where the beam is split into two parts, a neutral density filter is used to further attenuate the monitoring beam. In addition, a programmable shutter (D122, Uniblitz, Vincent Associates, Rochester, NY) is placed in the path of the photobleaching beam. A hole cut in the shutter ensures that the monitoring beam is always incident at the oil-water interface, leaving the photobleaching beam shuttered, except during the brief instances during which photobleaching is required.

The monitoring beam, whose power is approximately 15 μ W before entering the prism, provides a light level sufficient to excite the fluorophores at the interface without inducing

unacceptable levels of photobleaching. When the shutter is opened, the recombined photobleaching and monitoring beams strike the interface at the same location. The photobleaching beam, whose power is approximately 100 mW before entering the prism, provides a light level strong enough to photochemically destroy the fluorophores (photobleaching). A photobleaching pulse duration of 100 ms was used for most experiments.

The recombined beam is passed through a half wave polarizer (10RP02-12, Newport Corporation, Irvine, CA), to enable a choice of either horizontal or vertical polarization of the incident light. In addition, an optical chopper (SR540, Stanford Research Systems, Inc., Sunnyvale, CA) is available during lengthy experiments to reduce unintended photobleaching by the monitoring beam. The beam is directed to the interface via a series of mirrors and focused onto the interface using a plano-convex lens (f = 200 mm, Oriel Corporation, Stratford, CT). It strikes the interface within the experimental cell at an angle of 64°, measured normal to the interface.

Fluorescence emission is collected by a photomultiplier tube (PMT) through a microscope objective (440651, 32X, 0.4, Carl Zeiss, Inc., Thornwood, NY), which is focused on the interface using the method described in section 3.3.2. A narrow band filter (535DF35, 518-552 nm wavelength range, Omega Optical, Inc., Brattleboro, VT) is placed below the microscope objective so that only light within the wavelength range of the emitted fluorescence can reach the PMT. The light that passes through the filter is directed

through the microscope to the PMT where its intensity is measured and converted into a digital signal.

The experimental setup used in our lab for TIRF/FPR experiments is shown in Figure 3.1.

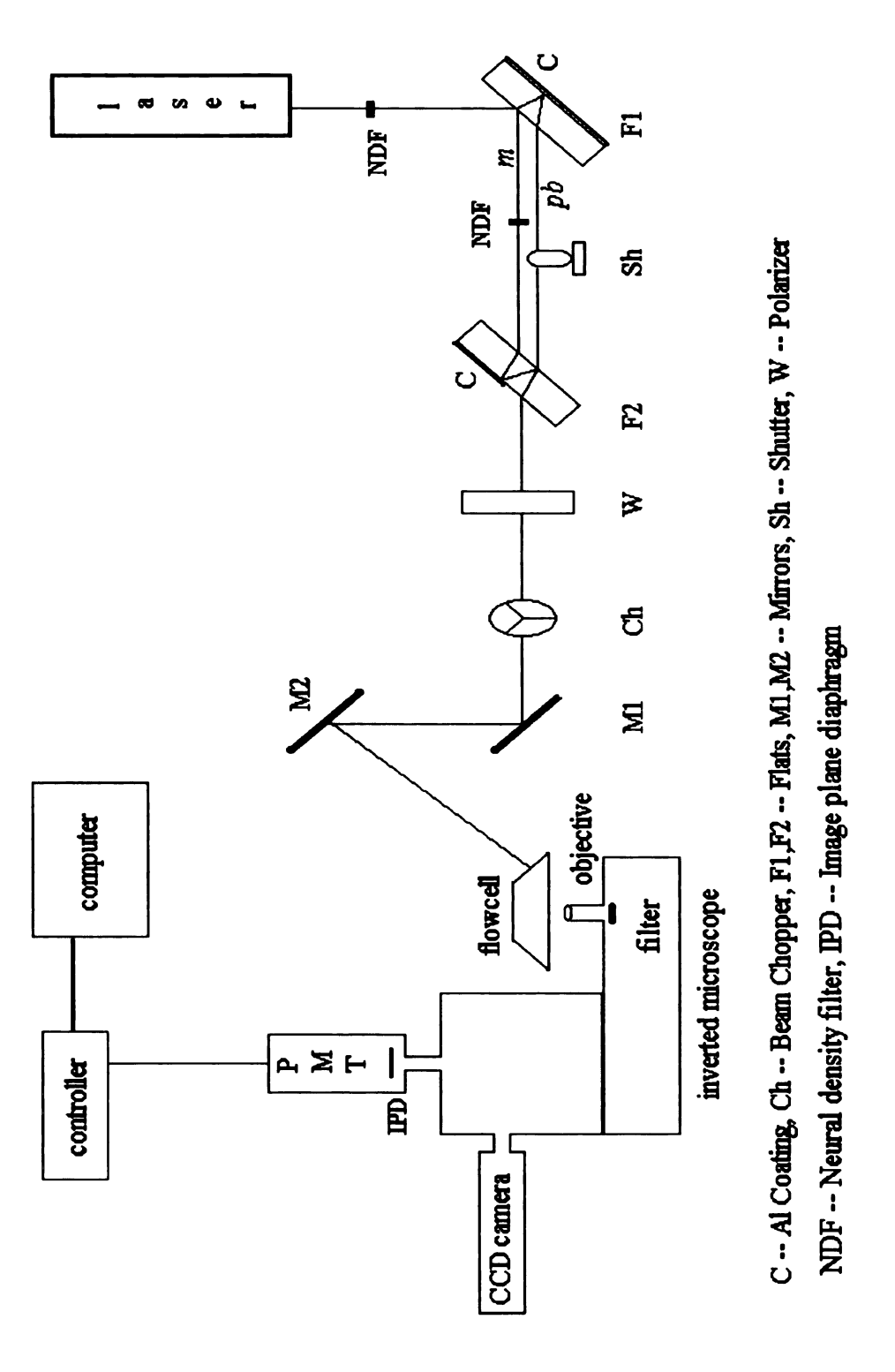


Figure 3.1: TIRF/FPR equipment. The laser beam is first split into photobleaching and monitoring beams and then recombined by optical flats before being directed to the oilwater interface. The PMT is used to collect the fluorescence emission.

3.2.2 The experimental cell

The experimental cell used in our lab for TIRF/FPR experiments is shown in Figure 3.2. A 64° dovetail prism is optically coupled to the top microscope slide (Fisher Scientific, Pittsburgh, PA) using an immersion oil (16482, type A, R.P. Cargille Laboratories, Inc., Cedar Grove, NJ). The underside of the top slide is coated (as described later in section 3.3.1) with the same oil to form the top half of the oil-water interface. Situated below the top slide is an aluminum spacer (1 mm thick) with a channel in the center to hold the water or protein solution which forms the bottom half of the oil-water interface. In this study, the terms "water" and "protein solution" are used interchangeably because the protein solution is composed mostly of PBS buffer, which in turn is made up mostly of deionized water.

An O-ring (Parker Seals, Lexington, KY) is placed around the perimeter of the spacer channel to prevent leakage of the protein solution. The bottom slide is coated with PEO, as discussed in section 3.1.2, and has two holes drilled in it to allow the inflow and outflow of protein solution from the double-syringe pump. After the cell is assembled as shown in the side view of Figure 3.2, the assembly is held in place by screwing it onto an anodized aluminum shell that sits on top of the microscope stage. The cell is sometimes referred to as a "flowcell," but it should be noted that flow is induced only during the infusion of buffer or protein solution into the cell. All TIRF/FPR experiments in this study were performed under stopped-flow conditions.

Side view of closed cell:

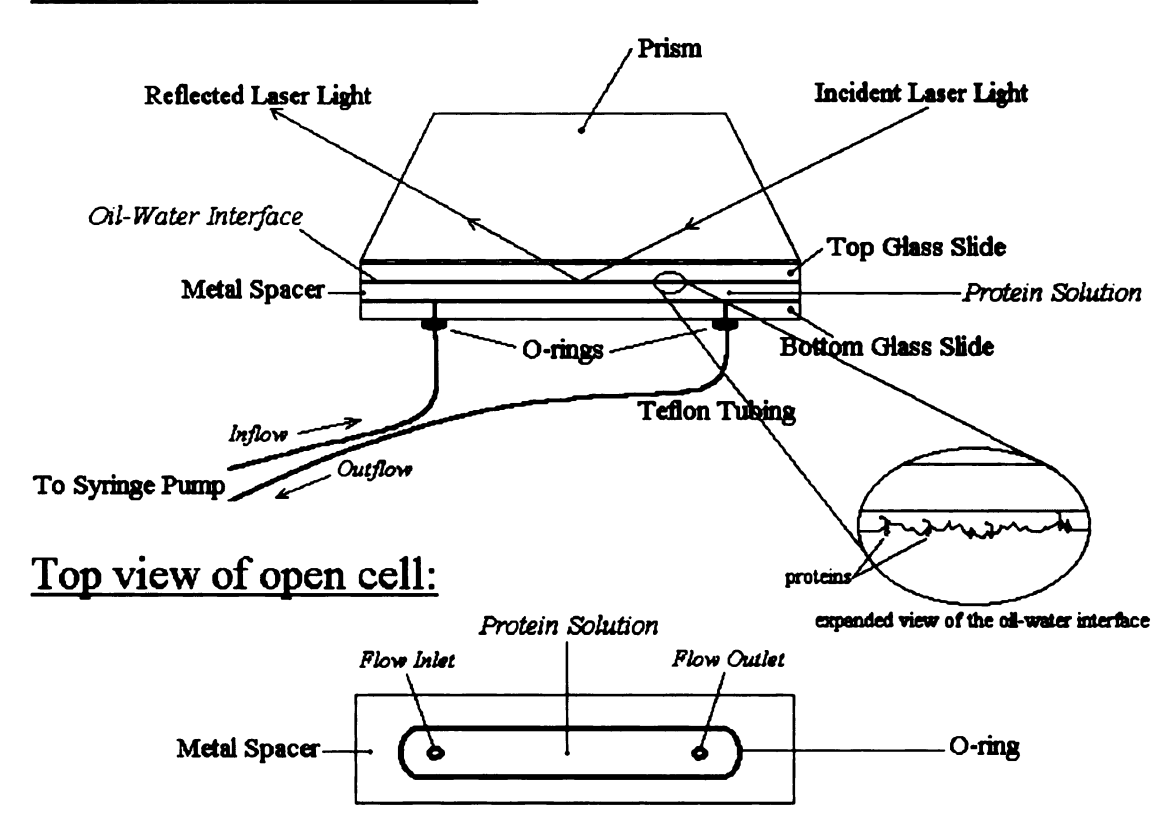


Figure 3.2: The experimental cell, or "flowcell." Note that the top view shows an "open" cell, meaning that the prism and top slide have been removed to give an internal view of the cell.

3.3 Experimental techniques

3.3.1 The oil-water interface

The structure of the oil-water interface should be as reproducible as possible to ensure that experiments are conducted under similar conditions. A different slide coating technique than was used by Jauhari (1997) was implemented to better fulfill this important criterion. A top slide (1 inch x 3 inches) was cleaned using the procedure described by Cheng et al. (1987). A drop of the immersion oil described in section 3.2.2 was then placed at one end of the slide, along its one-inch dimension. A cylindrical glass rod was smoothly dragged over the slide, thereby sweeping the surface of the slide and evenly coating it with oil. The oil layer was estimated to be approximately 80 µm thick by weighing multiple slides before and after coating. Since the cell has a total depth of 1 mm, the protein solution is estimated to be 920 µm thick. Jauhari (1997) found that this depth is thin enough to give an equilibrium adsorption time on the order of minutes.

Once the oil half of the interface has been formed on the top slide, the other side of the slide is optically coupled to the prism using the same oil. The prism-slide assembly is then placed, slide side down, on top of the cell, which has been pre-filled with protein solution (the water half of the interface), to form the oil-water interface.

The protein solution is introduced into the cell using a two-step process. First, the solution is pipetted into the open cell. The cell is then sealed by placing the prism-slide assembly on top of it. Small air bubbles sometimes get trapped in the cell during the

process of sealing it. The air bubbles are subsequently removed by pumping additional protein solution into the cell, using a double-syringe pump system which simultaneously infuses and withdraws fluid from the cell. The exit port of the cell has been designed to effectively aid the removal of trapped air bubbles.

We have always exercised appropriate caution when using the syringe pump, because of the possibility of shearing oil and/or adsorbed proteins off the interface as fluid flows through the cell. Jauhari (1997) reported that, for our experimental apparatus, a flow rate of 0.17 mL/min can be safely used without damaging the oil-water interface or sweeping adsorbates away. As an added precaution, we used flow rates no higher than 0.05 mL/min. Additionally, all desorption experiments were performed under stopped-flow conditions.

3.3.2 Focusing of microscope objective at the liquid-liquid interface

Focusing the microscope objective on the oil-water interface has been a challenge since the beginning of our studies. There was no reproducible method of getting a proper focus, because the oil-water interface provides no landmark on which to focus, and the oil layer cannot be guaranteed to be the same thickness for different constructions of the oil-water interface. Studies involving the solid-liquid interface achieve proper focus by placing a mark, such as a small dot, on the slide and visually focusing the microscope on that point. Jauhari (1997) previously attempted to focus using a visual technique, but the qualitative nature of this technique could not assure a reproducible focus.

As a result, devising and implementing a precise method of focusing the microscope objective at the oil-water interface was a key activity for this study. Several experiments showed that poor focusing could lead to an inability to detect fluorescence recovery after photobleaching.

Zimmerman et al. (1990) observed that the exchange of proteins within the bulk occurs at a faster rate than the time resolution of the experiment. In other words, proteins within the bulk exchange rapidly enough that a fluorescence recovery profile will not be observed in the experimental data; instead, the fluorescence intensity will apparently return instantaneously to the pre-bleach level. This is apparent in Figure 3.3, which shows a photobleaching experiment in which the microscope objective has been focused in the bulk aqueous phase instead of at the interface. About 15 seconds into the run, a photobleaching pulse is observed in the form of a sharp increase in the signal. When the pulse ends, the fluorescence signal returns instantaneously to the pre-bleach level, indicating that the fluorescence recovery occurs too rapidly for our data acquisition system to resolve a recovery curve.

It should be noted that this type of situation can also occur when the spot being photobleached is not properly centered in the field of view. Therefore, both proper laser beam alignment and precise focusing of the microscope objective are essential to obtaining useful post-photobleaching recovery profiles.

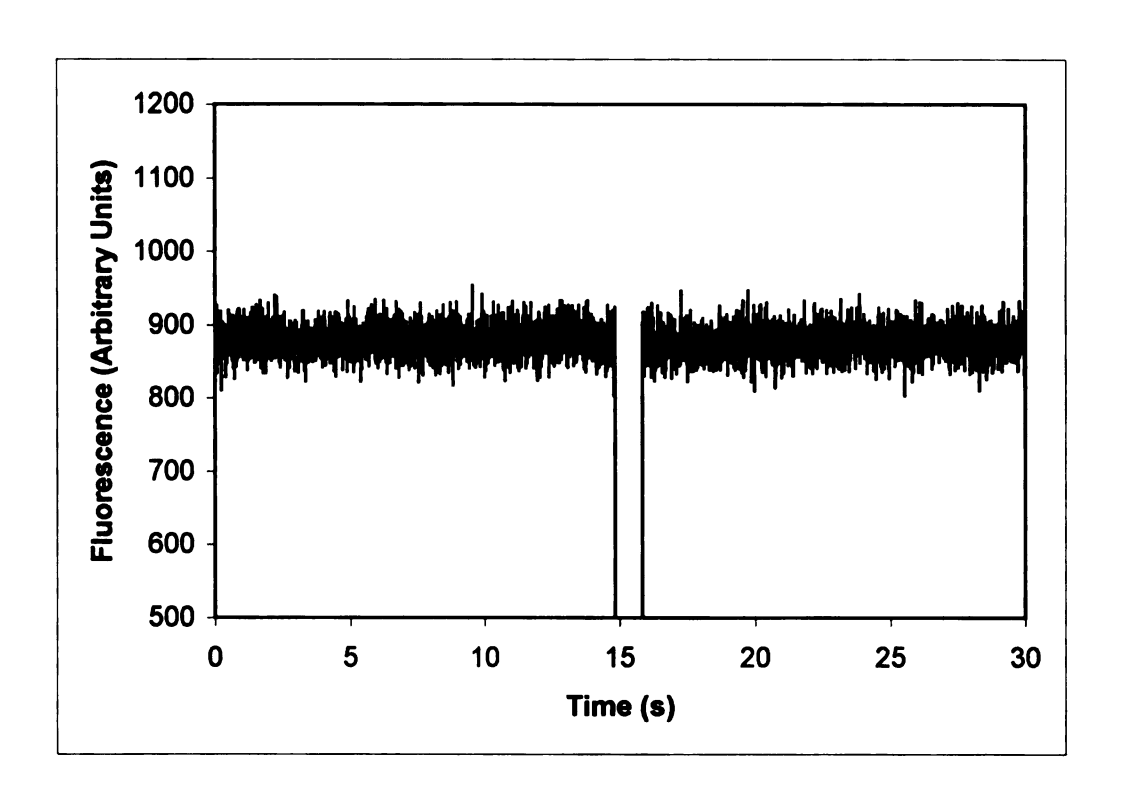


Figure 3.3: TIRF/FPR experiment showing one effect of improper focusing of the microscope objective. A photobleaching pulse occurs at time 15 seconds, but no post-bleaching drop in intensity is observed, because the microscope objective is focused in the bulk protein solution, rather than at the oil-water interface.

We have developed a new technique to obtain a more reliable and reproducible focus of the microscope objective on the oil-water interface. We take advantage of the fact that the intensity of the evanescent wave is highest at the oil-water interface, which is where we want the objective to be focused. With the monitoring beam striking the interface, the microscope objective is moved to its highest point, so that it will be focused above the interface. The objective is then moved downward in small increments, and the light level is checked at each increment. As the objective gets progressively lower, the light level increases quickly and then reaches a maximum. The light level decreases as the objective is lowered further, indicating that the oil-water interface has been passed. Moving the microscope objective back to the initial point of the highest fluorescence signal allows us to obtain a reliable and reproducible objective focus at the interface.

3.3.3 Fluorescence photobleaching recovery (FPR)

FPR has been used extensively to study the kinetics of desorption at a solid-liquid interface (Thompson *et al.* 1981; Burghardt and Axelrod 1981; Pearce *et al.* 1991; Pisarchick and Thompson 1991; Hellen and Axelrod 1991; Abney *et al.* 1992; Pisarchick *et al.* 1992). The same technique is used in this study, essentially without modification, as described below.

Labeled proteins at a spot on the oil-water interface fluoresce due to excitation energy from the evanescent wave created by the monitoring beam. A brief pulse (100 ms for most experiments) of the photobleaching beam strikes the same spot on the interface,

photobleaching the fluorophores at and near the interface and causing a drop in fluorescence signal. The recovery of the fluorescence signal towards the pre-bleach level is monitored, as photobleached molecules desorb from the interface and are replaced by unbleached molecules from the bulk solution.

In a typical TIRF/FPR experiment, 5000 data points are taken at a rate of 82 data points per second, corresponding to an experimental run time of about one minute. Each data point is an average of 256 readings from the photomultiplier tube. Approximately 10 seconds after the data acquisition has begun, a 100 ms photobleaching pulse impinges on the spot being monitored, causing the fluorophores at and near the interface to be photobleached. The remaining 50 seconds of data acquisition records the recovery of fluorescence due to exchange of bleached molecules at the interface with unbleached molecules from the bulk.

A competing factor in this process is the decrease in fluorescence over time due to a slow photobleaching of fluorophores at and near the interface. This is a result of the continuous impingement of the monitoring beam at the interface. If this becomes significant, then it must also be taken into consideration in data analyses, as explained in Chapter 4, section 4.2

4. ANALYSIS TECHNIQUE

4.1 A biexponential trend in the kinetics of desorption

Under reaction limited conditions, fluorescence recovery after photobleaching is controlled by the rate of desorption of photobleached proteins from the interface, and it can be described by the following monoexponential equation (Thompson *et al.* 1981):

$$F(-) - F(t) \approx [F(-) - F(0)]e^{-k_d t}$$
 [14]

However, studies using both BSA (Burghardt and Axelrod 1981) and other proteins (Pearce et al. 1992; Pisarchick et al. 1992) have shown that recovery curves from TIRF/FPR experiments in the reaction limited regime are best described by two exponential desorption terms. Equation [14] can thus be rewritten in biexponential form as (Burghardt and Axelrod 1981):

$$F(-) - F(t) = [F(-) - F(0)](r_0 + r_1 e^{-k_1 t} + r_2 e^{-k_2 t})$$
 [15]

where

$$r_0 + r_1 + r_2 = 1$$
 [16]

and k_1 and k_2 represent the apparent rapid and slow rates of desorption, respectively (Burghardt and Axelrod 1981).

The parameters r_1 and r_2 represent the fraction of proteins that desorb according to rate constants k_1 and k_2 , respectively. The fraction of proteins that are irreversibly adsorbed to the interface (the immobile fraction) is given by r_0 . Therefore, the mobile fraction, f, is given by

$$f = 1 - r_0 = r_1 + r_2 \tag{17}$$

4.2 Accounting for slow photobleaching due to the monitoring beam

In an ideal situation in which photobleaching due to the monitoring beam does not occur, Eqn. [15] is adequate to model fluorescence recovery in TIRF/FPR experiments. In practice, however, a decay in signal level occurs, due to the continuous excitation of fluorophores by the monitoring beam. This decay can be described by an exponential function (Hirschfeld 1976; Wells *et al.* 1989, Song *et al.* 1995) of the form

$$F(t) = F(0)e^{-k_{pb}t}$$
 [18]

where k_{pb} is the rate constant describing photobleaching due to continuous fluorophore excitation by the monitoring beam.

We conducted experiments in which the monitoring beam was allowed to continuously excite fluorophores at and near the oil-water interface and measured an average k_{pb} value of approximately 8×10^{-4} s⁻¹. At this rate, the fluorescence level drops by about 5% over a period of 60 seconds. Since a drop in the fluorescence signal will counteract the effects of fluorescence recovery after spot photobleaching (FPR), we had to modify Eqn. [15] to ensure that the effects of both desorption and photobleaching are accounted for. The modified equation is

$$F(-) - F(t) = \left[F(-) - F(0) e^{-k_{pb}t} \right] \left(r_0 + r_1 e^{-k_1 t} + r_2 e^{-k_2 t} \right)$$
[19]

For this equation to be valid, it must reduce to Eqn. [15] in the limit as k_{pb} approaches zero; it must also reduce to Eqn. [18] in the limit as both k_1 and k_2 approach zero. It can be readily verified that these limits are met by Eqn. [19]. Further verification of Eqn. [19] can be based on comparing the value of k_{pb} obtained in experiments for which no photobleaching pulse is used (i.e. curve fitting data to Eqn. [18]) to the value of k_{pb} obtained in TIRF/FPR experiments (i.e. curve fitting data to Eqn. [19]). As will be discussed further in Chapter 5, the average k_{pb} value obtained by using both methods was approximately 8×10^{-4} s⁻¹, further confirming the validity and appropriateness of using Eqn. [19].

4.3 Analysis of TIRF/FPR data

Fluorescence data are collected as described in section 3.3.3. The first 10 seconds of the data (prior to impingement of the photobleaching beam) give the pre-bleach fluorescence intensity, F(-). Time t = 0 is defined as the time at which the photobleaching pulse is terminated and fluorescence recovery begins. F(0) is the fluorescence intensity at time t = 0 and can be obtained directly from the experimental data or can be determined in the curve fitting procedure.

Using the graphing program SigmaPlot (Jandel Corporation, San Rafael, CA), the recovery data starting at t = 0 is fit to Eqn. [19], using a nonlinear regression procedure. The routine takes the experimental data of F(t) versus t and obtains a best fit curve by

iterating from initial guesses of F(0), r_0 , r_1 , r_2 , k_1 , k_2 , and k_{pb} values. The iterative process is subject to two constraints: a) Eqn. [16] must be satisfied, and b) all the estimated parameters must have non-negative values, because (as Eqn. [19] is written), negative parameters have no physical meaning.

5. RESULTS AND DISCUSSION

5.1 Desorption kinetics of BSA-FITC at an oil-water interface

Four important features (or periods) can be extracted from the fluorescence recovery curves for the desorption of BSA-FITC molecules from the oil-water interface. The first is a period of fast initial recovery, which is indicative of a fraction (r_1) of molecules that desorb rapidly from the interface at an apparent rate k_1 . The second feature is a period of slower recovery, which indicates a fraction (r_2) of molecules that desorb at a slower rate (k_2) . The third feature is a fraction (r_0) of molecules that are irreversibly adsorbed at the interface. It is important to note that "irreversibility" in this sense only applies over the observation time of the experiment, and that a nearly complete fluorescence recovery may be seen if the interface is monitored over several hours. Figure 5.1 shows these first three features.

The final important feature observed is a decay in fluorescence intensity due to the slow photobleaching of fluorophores at the interface, induced by the continuous impingement of the monitoring beam on the interface. This occurs at a rate k_{pb} , and its influence on the system becomes more pronounced at longer durations (on the order of 10^3 minutes). Figure 5.2 illustrates this final feature.

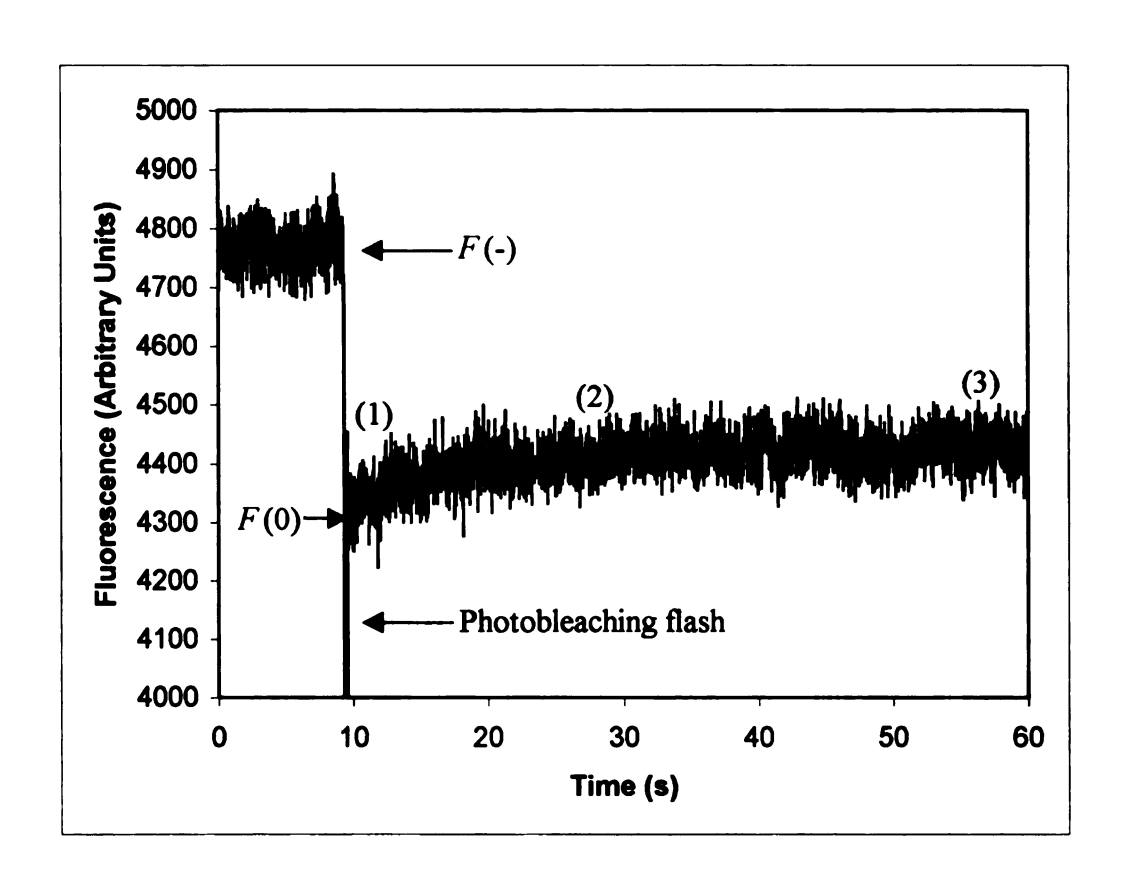


Figure 5.1: Typical fluorescence recovery curve for TIRF/FPR experiments. Initially, there is a fast recovery of fluorescence (1), which is followed by a slower period of recovery (2). The fluorescence does not completely recover to its pre-bleach level (3), indicating that a fraction of photobleached proteins are irreversibly adsorbed to the interface. F(-) is the equilibrium fluorescence prior to photobleaching, and F(0) is the fluorescence immediately after the photobleaching flash, which occurs approximately 10 seconds into the experiment and has a duration of 100 ms. The bulk protein concentration for this data was 0.04 mM.

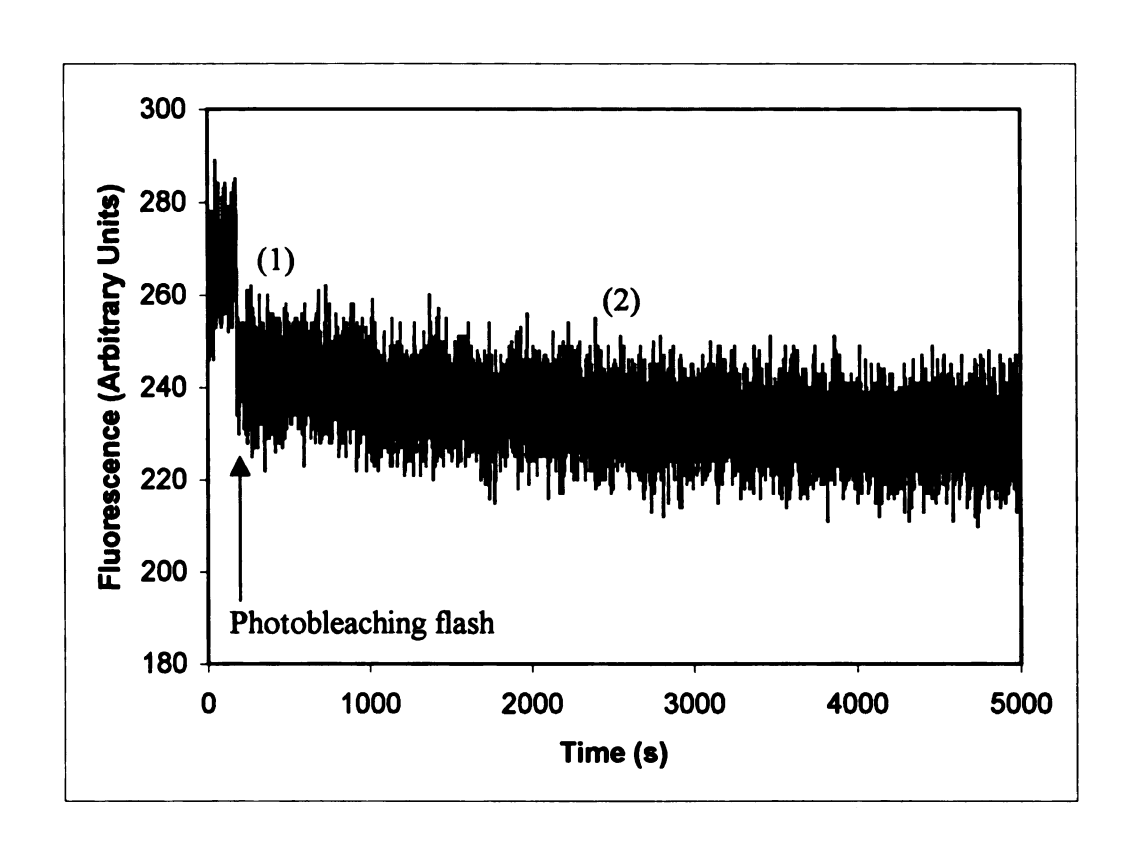


Figure 5.2: Drop in fluorescence during a long experiment, due to slow photobleaching by the monitoring beam. The fluorescence level abruptly drops after the photobleaching flash. A partial recovery of fluorescence occurs over a brief period (1), after which the fluorescence level slowly drops, due to unintended photobleaching (2). The bulk protein concentration for this data was 0.04 mM.

Table 5.1 and Table 5.2 show the kinetic desorption parameters calculated from the TIRF/FPR data. These variables were obtained by curve fitting the experimental data to Eqn. [19]. Figure 5.3 through Figure 5.8 show the results graphically as a function of bulk concentration. The error bars correspond to the standard deviations of the average values obtained for each parameter. Four BSA-FITC bulk concentrations were studied, ranging from 0.01 to 0.10 mM.

Burghardt and Axelrod (1981) showed that for bulk concentrations of BSA greater than or equal to 0.015 mM, fluorescence recovery is limited by desorption reaction kinetics rather than by bulk diffusion. For the system to be in the reaction limited regime, they showed that the following relationship must be satisfied:

$$\frac{R_{BND}}{k_d} \ge 20 \tag{20}$$

where R_{BND} is given by Eqn. [12].

To calculate R_{BND} , the concentration of proteins at the interface $[\overline{C}]$ must be known. Unfortunately, at the present time, we have no reliable technique for using fluorescence emission data to calculate the concentration of proteins at the liquid-liquid interface. Therefore, we have assumed that the ratios of interfacial to bulk protein concentrations at the liquid-liquid interface are comparable to those at the solid-liquid interface. Based on this assumption, we can use the criterion established by Burghardt and Axelrod (1981). Thus, we expect the desorption rates to stabilize as the bulk concentration goes above 0.015 mM, and we look for diffusional effects to become negligible.

Table 5.1: Summary of the apparent desorption and photobleaching rate constants for BSA-FITC at the oil-water interface.

Bulk Conc. (mM)	k ₁ (s ⁻¹)	k_2 (s ⁻¹)	k_{pb} (s ⁻¹)
0.01	0.20 ± 0.02	0.0015 ± 0.0004	0.0011 ± 0.0002
0.04	0.39 ± 0.15	0.008 ± 0.002	0.0009 ± 0.0003
0.07	0.52 ± 0.12	0.008 ± 0.003	0.0007 ± 0.0002
0.10	0.51 ± 0.09	0.009 ± 0.002	0.0006 ± 0.0003

Table 5.2: Values obtained for the immobile fraction (r_0) , and the fractions of proteins that desorb at rates k_1 and k_2 $(r_1$ and r_2 , respectively).

Bulk Conc. (mM)	r ₀	<i>r</i> ₁	<i>r</i> ₂
0.01	0.45 ± 0.07	0.098 ± 0.039	0.45 ± 0.03
0.04	0.51 ± 0.15	0.093 ± 0.008	0.40 ± 0.16
0.07	0.46 ± 0.04	0.091 ± 0.009	0.45 ± 0.05
0.10	0.38 ± 0.07	0.24 ± 0.02	0.38 ± 0.05

Figure 5.3 illustrates the dependence of the apparent rapid desorption rate constant k_1 (units of s⁻¹) on the bulk concentration. The biexponential desorption kinetic model we have used gives a consistently good fit to the experimental data, as it has been shown to do in studies of similar protein systems (Burghardt and Axelrod 1981; Pearce *et al.* 1992; Pisarchick *et al.* 1992). Given the level of noise and variability in the fluorescence recovery curves, adding a third desorption rate constant would likely not yield any more reliable or useful information about the adsorption and desorption processes.

In this study, we define k_1 as the apparent rate at which loosely adsorbed proteins desorb from the interface. Since the proteins are loosely bound to the interface, they can more readily desorb, and (as will be shown shortly) the k_1 values were about two orders of magnitude larger than those calculated for k_2 , which we classify as the apparent rate at which proteins adsorbed directly to the oil-water interface desorb from the interface.

Figure 5.3 shows that, as the bulk concentration goes above 0.01 mM and the reaction limited regime is reached, k_1 increases and appears to quickly stabilize. At a concentration of 0.01 mM (the first data point), the rate of fluorescence recovery is limited by bulk diffusive processes. As the bulk concentration is increased, bulk proteins near the interface are more readily available to exchange with proteins adsorbed at the interface, and the exchange becomes limited by the rate at which proteins can desorb from the interface and create room for arriving molecules.

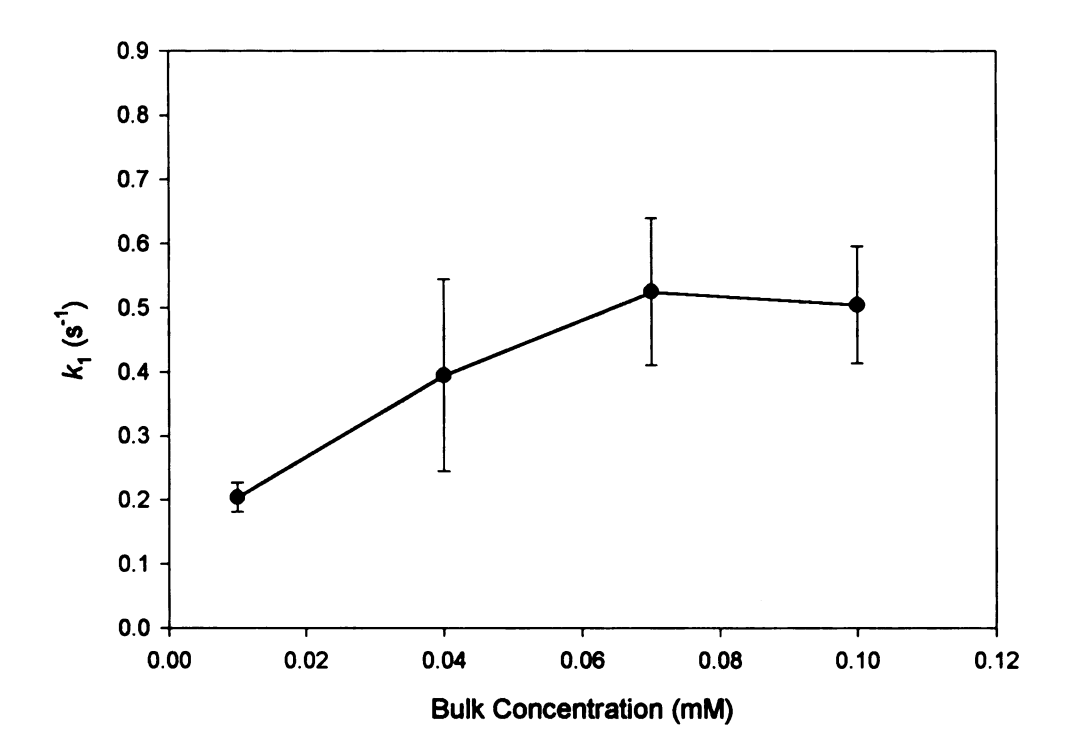


Figure 5.3: Apparent rapid desorption rate constant k_1 as a function of bulk protein concentration. Each data point represents the average of twenty experiments conducted at room temperature (~20°C) and in the dark. The photobleaching pulse duration was 100 ms.

Figure 5.4 illustrates the dependence of the apparent slow desorption rate constant k_2 (units of s⁻¹) on the bulk concentration. We define k_2 as the apparent rate at which proteins that are more tightly adsorbed to the oil-water interface desorb from the interface. As would be expected, these proteins desorb much more slowly than the proteins described by k_1 . For that reason, the k_2 values are about two orders of magnitude smaller than those of k_1 .

In spite of their quantitative differences, we see the same general trend in Figure 5.4 that was observed in Figure 5.3: as the bulk concentration goes above 0.01 mM and the reaction limited regime is reached, k_2 increases dramatically as it approaches an apparent but not well-established plateau. The value of k_2 increased fivefold as the bulk concentration increased from 0.01 mM to 0.04 mM. We interpret this as an indication that a transition between the diffusion and reaction limited regimes has most likely occurred, because the apparent rate of desorption is less limited by bulk protein diffusion.

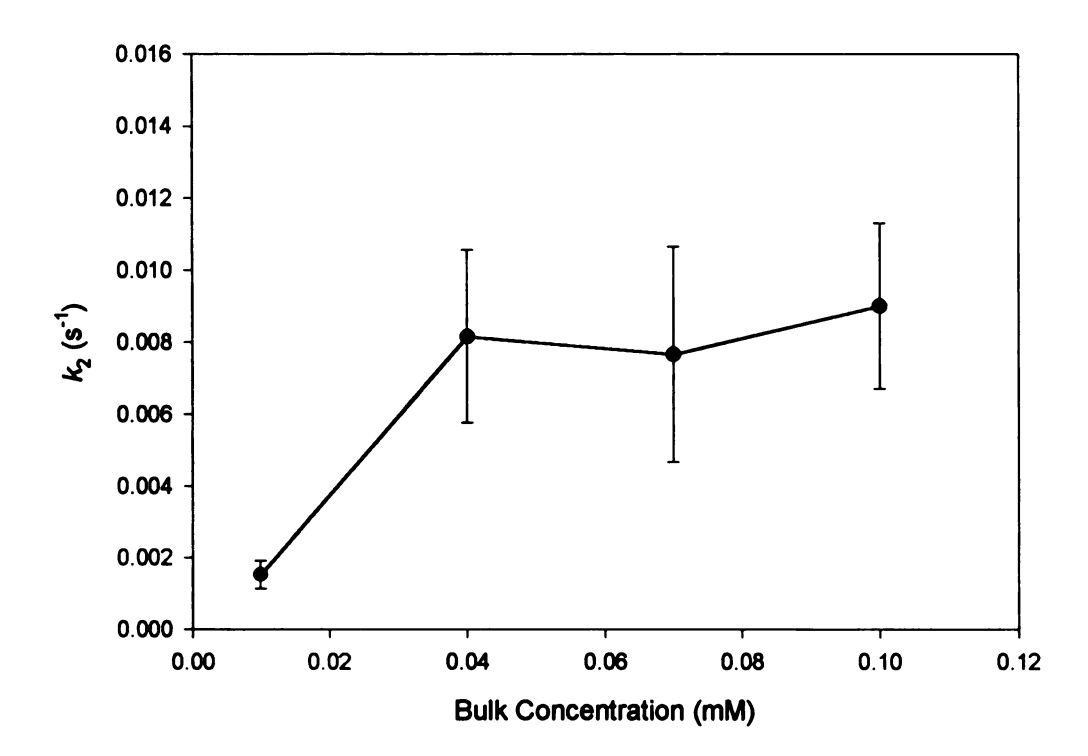


Figure 5.4: Apparent slow desorption rate constant k_2 as a function of bulk protein concentration. Each data point represents the average of twenty experiments conducted at room temperature (~20°C) and in the dark. The photobleaching pulse duration was 100 ms.

Figure 5.5 shows the values obtained for k_{pb} (units of s^{-1}), which measures the rate of slow unintended photobleaching caused by the monitoring beam. It should be noted that, for a given bulk concentration, the absolute value of k_{pb} depends on the monitoring beam intensity during the experiment. We conducted all experiments with a monitoring beam intensity of approximately 15 μ W (measured just before the beam enters the prism). More interesting than the absolute value of k_{pb} is the monotonic decrease in its value with increasing bulk concentration. This trend is to be expected because, as the bulk concentration increases, more fluorophores are available within the field of the evanescent wave at any given time. Therefore the average excitation energy imparted to an individual fluorophore decreases, accompanied by a corresponding decrease in the overall rate of photobleaching.

For the monitoring beam intensity used in our experiments, k_{pb} is on average about one order of magnitude smaller than the apparent slow desorption rate constant k_2 . Therefore, at first glance, it might seem unnecessary to include the effects of photobleaching in our data analysis. However, it will be shown later that the effects of slow photobleaching are significant, especially over longer experiments (on the order of 10^3 seconds).

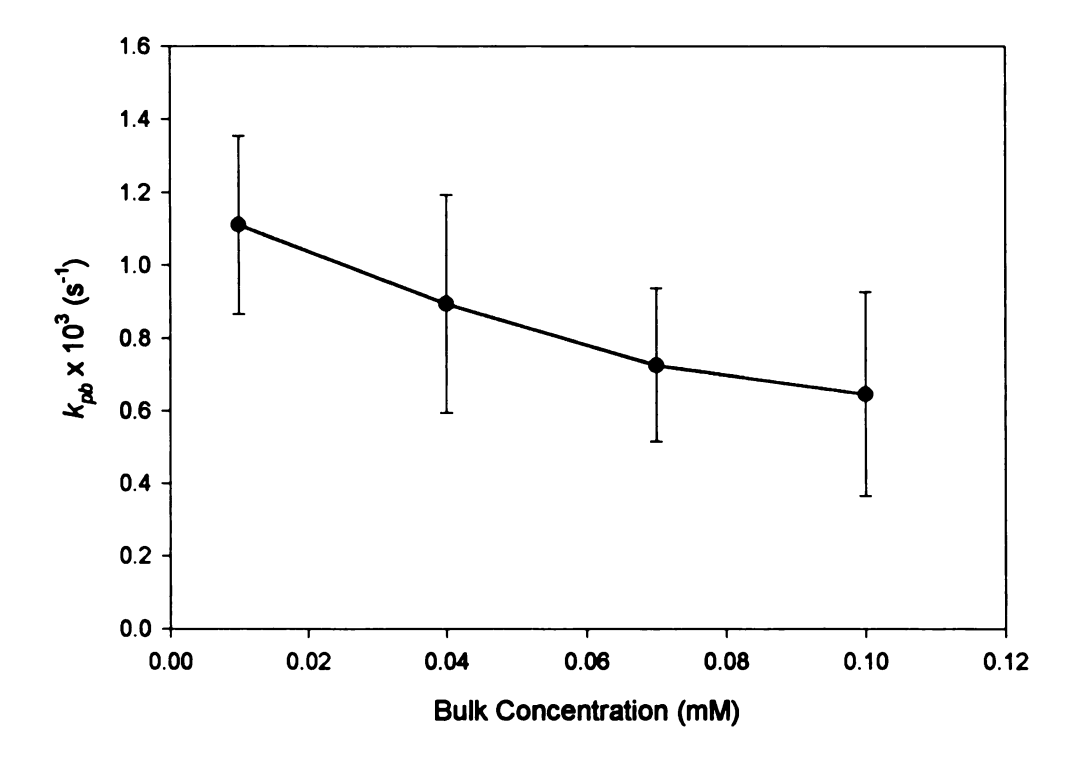


Figure 5.5: Slow photobleaching rate constant k_{pb} as a function of bulk protein concentration. Each data point represents the average of twenty experiments conducted at room temperature (~20°C) and in the dark. The photobleaching pulse duration was 100 ms.

Figure 5.6 shows the dependence of the immobile fraction r_0 on the bulk concentration. Although the trend is not monotonic, r_0 seems to decrease (within experimental uncertainty) with increasing bulk concentration. This trend was also observed by Burghardt and Axelrod (1981) for BSA adsorbed to a glass-water interface. Burghardt and Axelrod (1981), however, observed r_0 values that were consistently higher for a given bulk BSA concentration than those obtained in this study at the oil-water interface. For example, at a bulk concentration of 0.10 mM, they obtained an r_0 value of about 0.5 (Burghardt and Axelrod 1981), compared to the value of 0.38 \pm 0.07 obtained in this study.

This would appear to indicate that BSA molecules adsorb less irreversibly at an oil-water interface than at a glass-water interface, which is a reasonable explanation for the observation. One might claim that this is because an oil-water interface is less stable than a glass-water interface and its interfacial integrity is therefore more easily compromised. However, we have attempted to minimize vibrational effects by placing our experimental apparatus on an excellent vibration isolation table. In addition, we have designed our system to accommodate a thin oil layer (~80 µm) and a thin aqueous layer (~920 µm), both dimensions selected in our efforts to make the oil-water interface behave macroscopically like a solid-liquid interface. A more plausible explanation for the difference is that not accounting for the slow photobleaching due to the monitoring beam can lead to an overestimation of the immobile fraction. This will be discussed more fully later in this thesis.

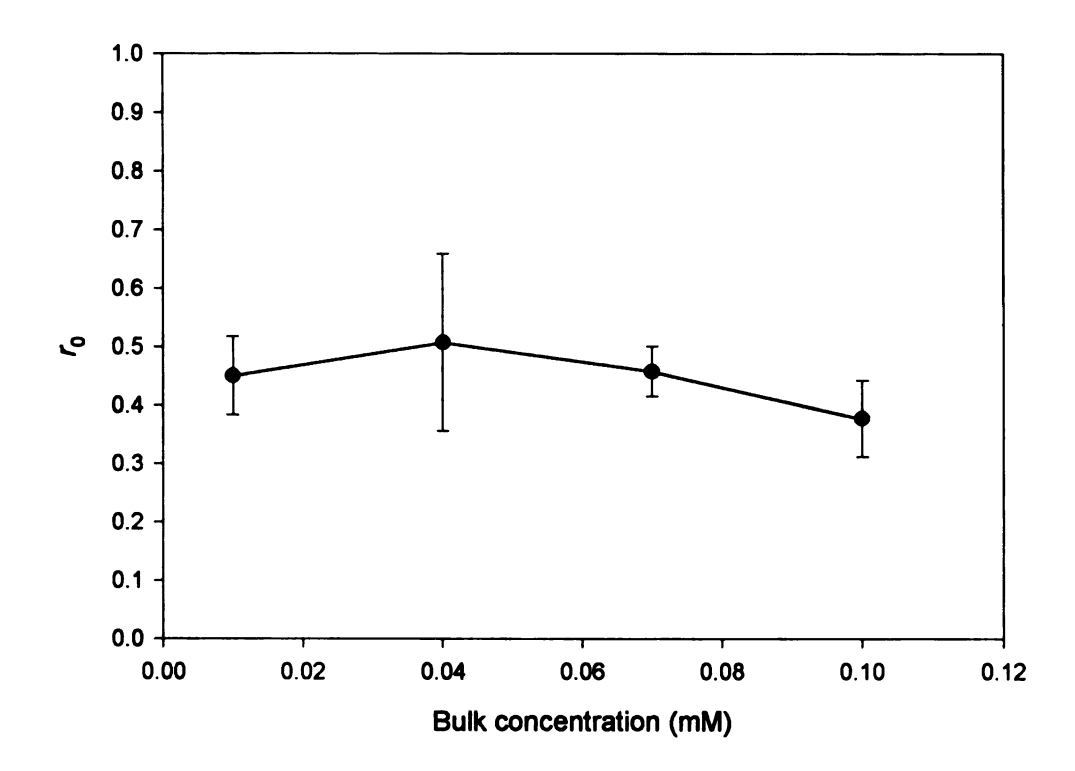


Figure 5.6: Immobile fraction r_0 as a function of bulk protein concentration. Each data point represents the average of twenty experiments conducted at room temperature and in the dark. The photobleaching pulse duration was 100 ms.

Figure 5.7 shows the dependence of r_1 , the fraction of proteins that desorb at rate k_1 , on the bulk concentration. The value of r_1 stays constant at about 0.09 for bulk concentrations between 0.01 mM and 0.07 mM, but an abrupt increase occurs between 0.07 mM and 0.10 mM. Burghardt and Axelrod (1981) did not observe this abrupt increase at 0.10 mM BSA-FITC at the solid-liquid interface but rather saw a steady increase in the value of r_1 with increasing bulk concentration. We currently do not have a reasonable explanation for the increase, but it is likely not due to differences between the interface used in this study and that used by Burghardt and Axelrod (1981).

Figure 5.8 shows the dependence of r_2 , the fraction of proteins that desorb at rate k_2 , on the bulk protein concentration. Within experimental uncertainty, r_2 is relatively constant with respect to bulk concentration. Burghardt and Axelrod (1981) observed an increase in r_2 with increasing bulk concentration. Such a trend might have been observed in this study had we not encountered the abrupt increase in r_1 between bulk concentrations of 0.07 mM and 0.10 mM. The absence of this abrupt increase in r_1 would increase r_2 at 0.10 mM above its current value of 0.38 \pm 0.05.

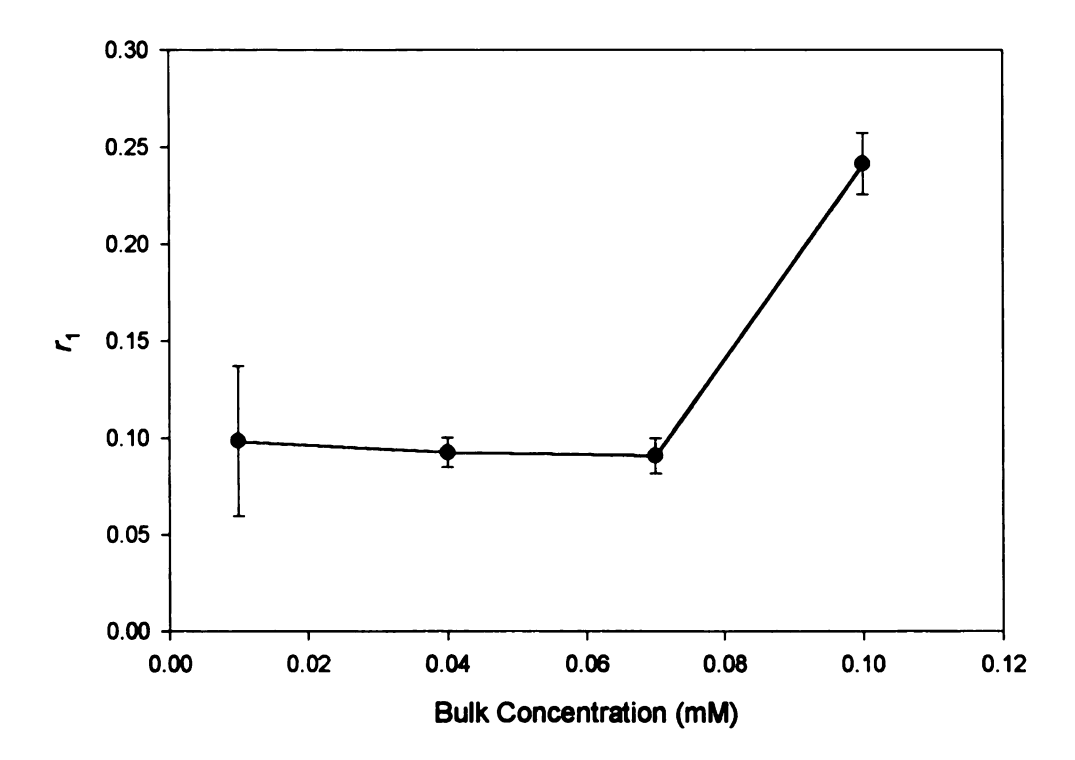


Figure 5.7: Fraction of proteins (r_1) that desorb at an apparent rate of k_1 , as a function of bulk protein concentration. Each data point represents the average of twenty experiments conducted at room temperature ($\sim 20^{\circ}$ C) and in the dark. The photobleaching pulse duration was 100 ms.

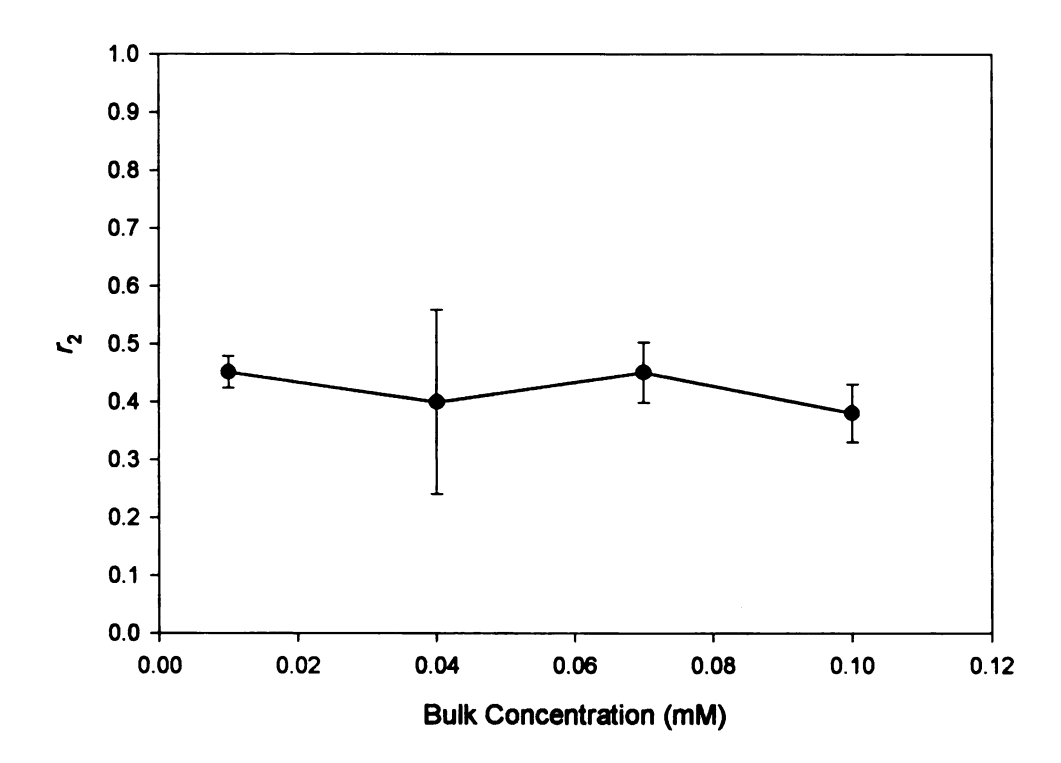


Figure 5.8: Fraction of proteins (r_2) that are more tightly held at the interface and desorb at an apparent rate of k_2 as a function of bulk protein concentration. Each data point represents the average of twenty experiments conducted at room temperature (~20°C) and in the dark. The photobleaching pulse duration was 100 ms.

Figure 5.9 and Figure 5.10 show theoretical fluorescence recovery curves based on the kinetic parameters obtained via curve fitting of experimental data to Eqn. [19] (see Chapter 4), at a bulk concentration of 0.07 mM. The parameters used are in the third row of data in Table 5.1 and Table 5.2. The dashed line in Figure 5.9 is qualitatively comparable to the experimental data shown in Figure 5.1, and the dashed line in Figure 5.10 is qualitatively comparable to the experimental data shown in Figure 5.2. Note that Figure 5.1 and Figure 5.2 represent data from single experimental runs, whereas the dashed lines in Figure 5.9 and Figure 5.10 were calculated from parameters obtained through the analysis of several experimental runs. Thus, we do not expect a quantitative match between Figure 5.1 and Figure 5.9 or between Figure 5.2 and Figure 5.10.

The solid lines in Figure 5.9 and Figure 5.10 represent theoretical calculations of what the experimental data would look like if slow photobleaching due to the monitoring beam did not occur. These lines were calculated by setting k_{pb} equal to zero in Eqn. [19]. As Figure 5.9 shows, the effect of slow photobleaching is noticeable but not significant during the first minute of fluorescence recovery. However, as is evident from Figure 5.10, the effects of slow photobleaching become very significant over longer experimental runs. In fact, the fluorescence level (dashed line) begins to drop at about 160 seconds. This has profound implications for TIRF/FPR experiments run over long times, as will be discussed further in section 5.2. The immobile fraction $[r_0]$ is the most drastically affected parameter. At a bulk protein concentration of 0.07 mM, r_0 was found to be 0.78 when slow photobleaching effects are neglected, compared to the actual r_0 value of 0.46 \pm 0.04 obtained in this study. This is discussed in further detail in Chapter 6.

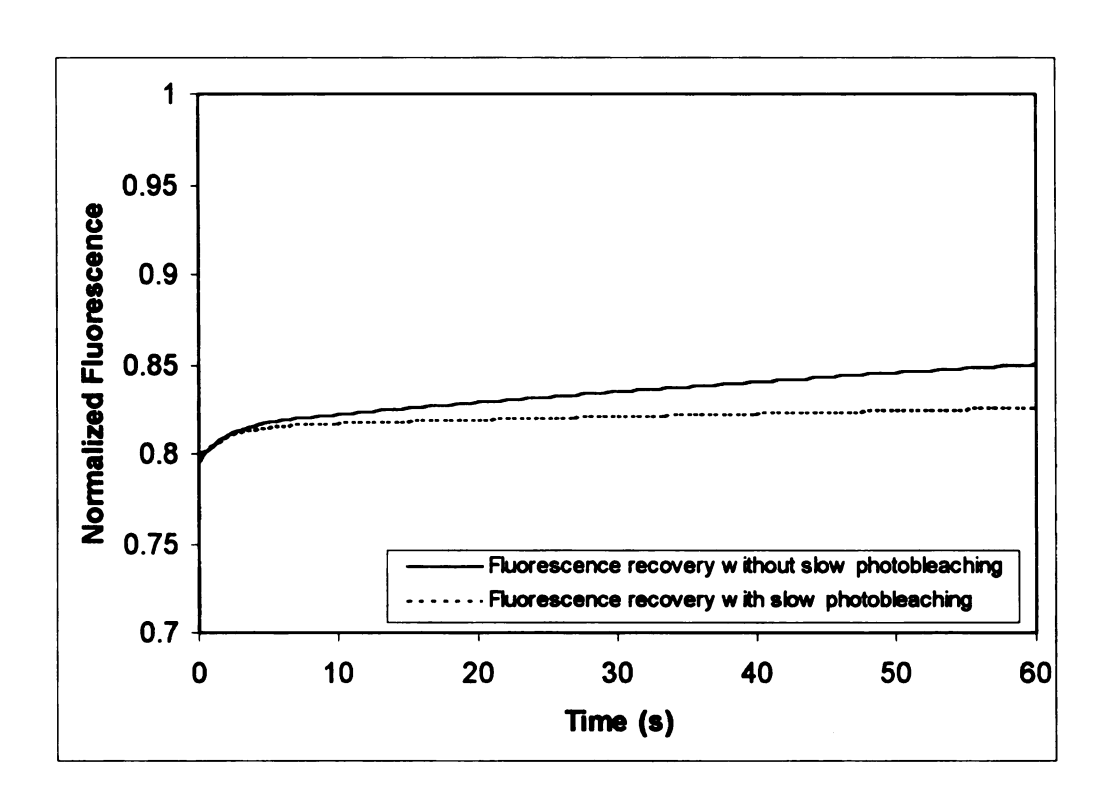


Figure 5.9: Short-term theoretical recovery curves generated from Eqn. [19], using the kinetic parameters obtained via curve fitting. The bulk concentration is 0.07 mM. The curve that assumes absence of slow photobleaching was generated by setting k_{pb} equal to zero in Eqn. [19].

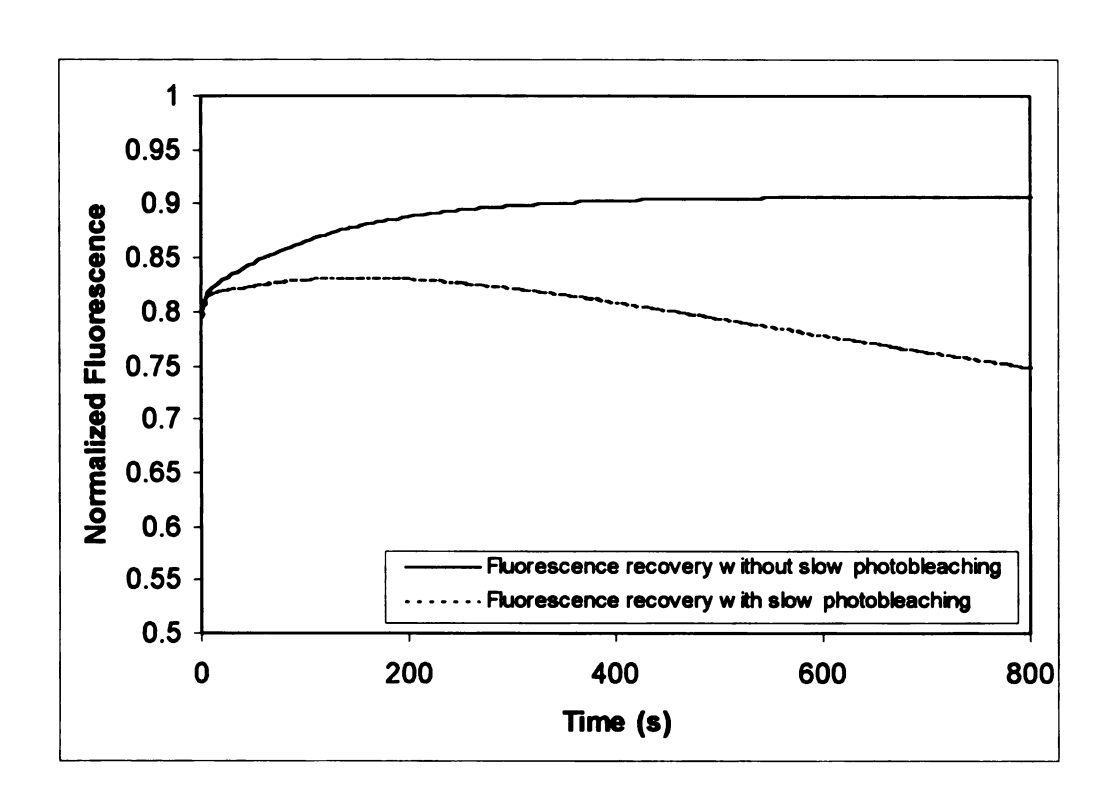


Figure 5.10: Long-term theoretical recovery curves generated from Eqn. [19], using the kinetic parameters obtained via curve fitting. The bulk concentration is 0.07 mM. The curve that assumes absence of slow photobleaching was generated by setting k_{pb} equal to zero in Eqn. [19].

5.2 Discussion

We have shown that slow photobleaching due to a continuously impinging monitoring beam can significantly influence fluorescence recovery data in TIRF/FPR experiments. We were able to account for this effect by estimating a slow photobleaching rate constant k_{pb} . There are two methods of obtaining k_{pb} : a) we can conduct experiments in which the monitoring beam is allowed to continuously excite fluorophores at and near the oilwater interface and fit the data to Eqn. [18], or b) we can run TIRF/FPR experiments and fit the data to Eqn. [19]. Within experimental uncertainty, the values obtained for k_{pb} with these two methods were identical, suggesting that protein adsorption/desorption is not coupled to slow photobleaching.

It is desirable to minimize the effects of slow photobleaching in experiments that run over long periods of time. For example, a study of protein adsorption onto a clean (protein free) interface would require monitoring the increase in fluorescence over a long period of time as the protein solution is pumped into the experimental cell to slowly displace buffer solution already in the cell. Unfortunately, we cannot use Eqns. [18] and [19] to account for the effects of slow photobleaching in systems with flow, because the equations apply only to systems in which there is no forced convection at or near the interface. Since we cannot mathematically account for slow photobleaching effects in systems with flow, we must explore methods to minimize the rate of slow photobleaching in such systems.

Slow photobleaching of fluorophores inevitably occurs when the monitoring beam strikes the interface, with the rate of photobleaching depending mainly on the beam intensity for a given bulk concentration. Reducing the monitoring beam intensity is often not a viable solution because the signal to noise ratio decreases. Alternatively, an optical chopper can be used during lengthy experiments to reduce the rate of unintended photobleaching. If a chopper does not sufficiently reduce the rate of photobleaching, a timed shutter system can be employed in which the monitoring beam is allowed to intermittently strike the interface. A trade-off must then be made between the percentage of experimental time that the monitor beam strikes the interface (i.e. the percentage of acquired data that is relevant) and the rate at which slow photobleaching occurs.

For lengthy experiments in which a slow, monotonic increase in fluorescence is expected, the shuttering method can be used. However, for experiments such as TIRF/FPR, the shuttering technique would be more difficult to implement. In a TIRF/FPR experiment, capturing the initial data points immediately following the photobleaching flash is crucial to obtaining an appropriate value for k_1 , because the rapid initial recovery described by k_1 is only observable in the first few seconds after photobleaching. A poorly timed shutter could cause these initial data points to be missed.

By using BSA-FITC bulk concentrations greater than 0.015 mM, we were reasonably assured that bulk diffusional processes would not contribute significantly to fluorescence recovery. However, lateral diffusion of interface-adsorbed proteins could still contribute to the recovery. We circumvented this problem by using a photobleaching beam whose

diameter is approximately three times that of the monitoring beam. Jauhari (1997) showed that, given the beam width and this ratio of diameters used in our apparatus, lateral diffusion of unbleached surface-bound fluorophores into the field of view of the monitoring beam occurs in about 900 seconds, which is much longer than the duration of our TIRF/FPR experiments.

In addition, once the microscope objective is properly focused at the interface, it sees only a small central portion of the monitoring beam spot. This may be confirmed by removing the photomultiplier tube and visually observing the elliptical spot made by the monitoring beam before and after proper objective focusing is achieved. When the microscope objective is not focused on the interface, the elliptical spot made by the monitoring beam is seen to cover only a small portion of the objective's field of view. As the focus gets closer to the interface, the elliptical spot covers more of the objective's field of view until, finally, only the central part of the spot can be seen as a proper focus is achieved. The time for unbleached surface-adsorbed proteins to laterally diffuse into the field of view of the microscope objective will then take even longer than 900 seconds.

5.3 Possible sources of error

We encountered noise and variability in the fluorescence recovery curves obtained in the TIRF/FPR experiments. The values of k_1 and k_2 appeared to be the most affected, as their relatively large errors of estimation would suggest (see Table 5.1, Figure 5.3, and Figure 5.4). A possible explanation is that the system was not given sufficient equilibration time

between experimental runs. Jauhari (1997) showed that, for the experimental apparatus used in our study, BSA-FITC reaches equilibrium approximately five minutes after the proteins have been pumped into the experimental cell. We allowed the system to equilibrate for at least 10 minutes after pumping stopped, so we do not believe insufficient equilibration time is a significant issue.

While inconsistent microscope alignment and focusing could hinder reproducibility, the monitoring beam has been found to maintain proper alignment for long periods of time (on the order of days), as has a proper focus of the objective at the oil-water interface. The use of a vibration isolation table to dampen vibrations from external sources helps maintain the integrity and stability of the oil-water interface, which in turn helps maintain the alignment and focus of the microscope objective. We can thus eliminate these factors as significant sources of error.

Internal noise from the PMT accounts for less than 5% of the fluorescence signal in typical TIRF/FPR experiments, and this background noise is stable over long periods of time, so it can also be eliminated as a significant source of error.

At the present time, the signal to noise ratio of our system is not high enough to distinguish minor factors such as rotational diffusion and structural unfolding of proteins as they adsorb to the interface. It is possible that with improvements in the signal to noise ratio, additional physically identifiable parameters could be added to the kinetic model, which would potentially improve the model's ability to repeatably predict experimental

data. At the current noise level of our experimental system, a biexponential kinetic model gives the best fit to TIRF/FPR data without overspecifying the system. This study has added the slow photobleaching rate constant, k_{pb} , to the biexponential kinetic model to improve the model's predictive ability.

6. SUMMARY AND CONCLUSIONS

We have established that a biexponential kinetic model fits TIRF/FPR data well and provides an acceptable framework for describing the desorption kinetics of BSA-FITC at the oil-water interface. Using two desorption rate constants, k_1 and k_2 , allows us to describe two types of desorbing proteins: k_1 is the apparent desorption rate of proteins loosely adsorbed at the interface, and k_2 is the apparent desorption rate of proteins adsorbed tightly at the oil-water interface. At a bulk protein concentration of 0.07 mM, k_1 was estimated to be 0.52 ± 0.12 s⁻¹, while k_2 had a value of 0.008 ± 0.003 s⁻¹. The noise and variability of the fluorescence recovery curves obtained in this study suggests that putting additional adjustable parameters into our current model would not add significant useful information about the system behavior.

Conducting experiments in the reaction limited regime assured us that bulk diffusional effects would not significantly affect the apparent rates of adsorption and desorption. Burghardt and Axelrod (1981) showed that, for the glass-water interface, bringing the bulk BSA-FITC concentration above 0.015 mM guarantees that the system is in the reaction limited regime. We assumed that a similar transition into the reaction limited regime would occur at the same concentration for the oil-water interface.

Figure 5.3 and Figure 5.4 provide evidence that a transition does indeed occur between bulk concentrations of 0.01 mM and 0.04 mM. Above 0.04 mM k_1 and k_2 reach reasonably stable levels that are no longer strongly dependent on concentration,

suggesting that bulk diffusional effects are not limiting the adsorption and desorption processes. Experimental uncertainty in the values of k_1 leaves open the possibility that the transition into the reaction limited regime could occur at a bulk concentration higher than 0.04 mM (see Figure 5.3). However, Figure 5.4 shows an abrupt transition between 0.01 mM and 0.04 mM as the value of k_2 jumps from 0.0015 \pm 0.0004 s⁻¹ to 0.008 \pm 0.002 s⁻¹ before stabilizing at that level. We conclude, therefore, that the transition between the bulk diffusion limited and reaction limited regimes for BSA-FITC at the oil-water interface occurs at approximately the same bulk concentration as at the glass-water interface.

Slow photobleaching due to the monitoring beam was found to have a significant effect on the fluorescence recovery curves obtained in our study. By adding the slow photobleaching rate constant k_{pb} to our mathematical model, we were able to successfully account for this factor. Two independent methods of determining k_{pb} (Eqns. [18] and [19]) yielded identical values, within experimental uncertainty.

As Figure 5.10 illustrates, slow photobleaching dominates the system behavior over long experimental periods. Initially, fluorescence increases due to the replacement of photobleached fluorophores at the interface by unbleached fluorophores from the bulk. As the rate of fluorescence recovery slows down over time, slow photobleaching causes the fluorescence signal to drop. In order to determine the effect of slow photobleaching on the kinetic parameters obtained in our study, we fit Eqn. [15] to the recovery curve predicted by Eqn. [19] at a bulk concentration of 0.07 mM (shown in Figure 5.9 as the dashed line).

The magnitudes of k_1 and k_2 were almost unchanged, as k_1 was found to be 0.51 s⁻¹ and k_2 was found to be 0.009 s⁻¹, compared to 0.52 \pm 0.12 s⁻¹ and 0.008 \pm 0.003 s⁻¹, the actual values obtained for a bulk concentration of 0.07 mM. The fraction of proteins which are loosely adsorbed at the interface, r_1 , also remained almost unchanged, with a value of 0.09. However, both r_0 and r_2 changed drastically: r_0 , the immobile fraction, was calculated to be 0.78 and r_2 was found to be 0.13, compared to 0.46 \pm 0.04 and 0.45 \pm 0.05, the actual values obtained for a bulk concentration of 0.07 mM.

We conclude from this that the main consequence of neglecting the effects of slow photobleaching is to overestimate the immobile fraction r_0 . Note that only the first 60 seconds of data were used in this exercise. Curve fits involving data from longer experiments in which slow photobleaching is more significant would most likely produce much larger errors in the values of k_1 and k_2 in addition to overestimating the immobile fraction.

7. SUGGESTIONS FOR FUTURE WORK

The goal of this thesis was to quantify the desorption kinetics of BSA-FITC at the oil-water interface. It serves as an important step towards using total internal reflection fluorescence to study more complex phenomena such as receptor-ligand interactions at the oil-water interface. Jauhari (1997) used the TIRF/FPR technique to study the surface and bulk diffusion coefficients of BSA-FITC at the oil-water interface, using the same basic experimental apparatus used in this study. This thesis builds on Jauhari's work by expanding the utility of TIRF/FPR as a tool to quantify the behavior of proteins at the oil-water interface. Modifications to our experimental setup are ongoing. A 70° dovetail prism will replace the 64° prism currently used. This will decrease the evanescent wave penetration depth (see Eqn. [3]), making the system more surface-selective. After this and other pending modifications are completed, we suggest that the following studies be conducted

7.1 Protein adsorption onto a clean interface

By slowly infusing a protein solution into the experimental cell of our TIRF/FPR apparatus (filled initially with the buffer used to make the protein solution) and monitoring the increase in fluorescence over time, quantitative information could be obtained about the kinetics of protein adsorption onto a clean oil-water interface. As is usual in such experiments, we would expect to see an initial flat fluorescence baseline, which would be characteristic of the "dead time" between the start of protein infusion and the arrival of

proteins into the field of view of the monitoring beam. The fluorescence signal would then increase steadily over time as protein molecules adsorb onto the interface. As the interface approaches saturation, there will be a decline in the rate of change of the fluorescence signal, and finally, the signal level will stabilize as the system reaches equilibrium.

Parameters describing the characteristics of the system, such as the dead time and the equilibration time, could be obtained. Several protein infusion rates could be used, and the change in fluorescence with time could be monitored for each infusion rate. These data would be useful in constructing a model for adsorption onto a clean interface that incorporates the effects of fluid flow. Infusion experiments could be conducted at several protein concentrations to yield information about the effect of concentration on the equilibration time.

The following precautions should be taken when conducting these experiments. The critical infusion rate at which shearing effects disrupt the integrity of the oil-water interface must not be exceeded. Jauhari (1997) reported this rate to be 0.17 mL/min for our apparatus. Slow photobleaching, which has been shown to be especially significant in lengthy experiments, would have to be dealt with. The most effective way to do this would be to employ a system in which the monitoring beam is shuttered so that it only strikes the interface periodically, during periods when data are being acquired. The optimum times for exposing and shuttering the monitoring beam could be determined experimentally. Criteria for this optimization are that slow photobleaching should be

minimized, while important trends in the data (such as the abrupt fluorescence increase when fluorophores reach the interface) must not be lost due to beam shuttering.

An additional concern regarding this study is that we are somewhat unsure about what fraction of the fluorescence signal comes from bulk proteins. Thus, it would be difficult to obtain an adsorption rate constant from these experiments, because part of the increase in fluorescence signal over time would come from the increase in bulk protein concentration during the infusion process. Currently, there is not a reliable technique for determining the surface concentration of proteins at the oil-water interface for a given bulk concentration.

The development of such a technique would enable us to calculate the ratio of bulk fluorescence to interfacial fluorescence, and knowing this ratio would enable us to include bulk diffusional effects in the determination of an adsorption rate constant. This ratio is given by $\overline{A}d/\overline{C}$, where \overline{A} is the bulk concentration, \overline{C} is the surface concentration (which we cannot presently determine), and d is the evanescent wave penetration depth, which is known. Burghardt and Axelrod (1981) reported that this ratio is 0.07 for the highest BSA-FITC concentration used in their study (techniques are readily available for determining surface concentrations at the solid-liquid interface), implying that at least 93% of the observed fluorescence is from surface adsorbed proteins. Until we can determine the surface protein concentration for a given bulk concentration, we cannot readily calculate an adsorption rate constant using protein infusion experiments. However, other useful information, such as the dependence of the dead time and the equilibration time on bulk concentration and infusion rate, can be readily determined.

7.2 Effect of labeling ratio on protein desorption kinetics

To study the effects of fluorescent labels on the behavior of proteins at the oil-water interface, the study conducted in this thesis could be expanded upon by conducting TIRF/FPR experiments at multiple labeling ratios. Robeson (1995) has reported that, as the labeling ratio is increased, elevated levels of concentration quenching accelerate the apparent recovery kinetics and cause the immobile fraction to be underestimated. As a result, concentration quenching would clearly have to be taken into account. The simplest way to circumvent the problem of concentration quenching is to use labeling ratios for which concentration quenching effects are not present. For BSA-FITC, concentration quenching was found to be absent for labeling ratios between 0.03-0.80 (Robeson 1995). For higher labeling ratios, Robeson (1995) has developed an analysis technique that takes into account the effects of concentration quenching on fluorescence recovery curves.

8. BIBLIOGRAPHY

- Abney, J.R., Scalettar, B.A. and Thompson, N.L. Evanescent interference patterns for fluorescence microscopy. *Biophys. J.* 61: 542-552 (1992).
- Arai, K., Kusu, F., and Takamura, K. Electrochemical behavior of drugs at oil/water interfaces. In: Liquid-Liquid Interfaces: Theory and Methods. 375-400 (1996).
- Axelrod, D. Cell-substrate contacts illuminated by total internal reflection fluorescence.

 J. Cell Biology 89: 141-145 (1981).
- Axelrod, D., Hellen, E.H., and Fulbright, R.M. In: Topics in Fluorescence Spectroscopy, Vol. 3: *Biomedical Applications*. Lakowicz, J.R. (ed.), 289-343 (1992).
- Burghardt, T.P. and Axelrod, D. Total internal reflection/fluorescence photobleaching recovery study of serum albumin adsorption dynamics. *Biophys. J.* 33: 455-468 (1981).
- Cheng, Y.L., Darst, S.A., Robertson, C.R. Bovine serum albumin adsorption and desorption rates on solid surfaces with varying surface properties. *J. Colloid Interface Sci.* 118: 212-223 (1987).
- Dickinson, E., Euston, S.R., and Woskett, C.M. Competitive adsorption of food macromolecules and surfactants at the oil-water interface. *Progr. Colloid. Polym. Sci.* 82: 65-75 (1990).
- Hellen, E.H. and Axelrod, D.J. Kinetics of epidermal growth factor/receptor binding on cells measured by total internal reflection/fluorescence recovery after photobleaching. J. Fluor. 1: 113-128 (1991).
- Hirschfeld, T. Quantum efficiency independence of the time integrated emission from a fluorescent molecule. *Appl. Opt.* 15: 3135-3139 (1976).
- Jauhari, P. A study of the diffusion of bovine serum albumin at the oil-water interface using total internal reflection fluorescence and fluorescence photobleaching recovery. M.S. Thesis, Michigan State University (1997).
- Lok, B.K., Cheng, Y.-L., and Robertson, C.R. Total internal reflection fluorescence: a technique for examining interactions of macromolecules with solid surfaces. *J. Colloid Interface Sci.* 91: 87-103 (1983a).

- Lok, B.K., Cheng, Y.-L., and Robertson, C.R. Protein adsorption on crosslinked polydimethyl siloxane using total internal reflection fluorescence. *J. Colloid Interface Sci.* 91: 104-116 (1983b).
- Pearce, K.H., Hiskey, R.G. and Thompson, N.L. Binding kinetics of fluorescently labeled bovine prothrombin fragment 1 at planar model membranes measured by total internal reflection fluorescence microscopy. *Biophys. J.* 59: 622a (1991).
- Pearce, K.H., Hiskey, R.G. and Thompson, N.L. Surface binding kinetics of prothrombin fragment 1 on planar membranes measured by total internal reflection fluorescence microscopy. *Biochemistry* 31: 5983-5995 (1992).
- Pisarchick, M.L, Gesty, D. and Thompson, N.L. Binding kinetics of an anti-dinitrophenyl monoclonal Fab on supported phospholipid monolayers measured by total internal reflection with fluorescence photobleaching recovery. *Biophys. J.* 63: 215-223 (1992).
- Pisarchick, M.L. and Thompson, N.L. Surface binding kinetics of a monoclonal Fab fragment on supported phospholipid monolayers measured by total internal reflection/fluorescence photobleaching recovery. *Biophys. J.* 59: 350a (1991).
- Robeson, J.L. Application of TIRF to probe surface diffusion and orientation of adsorbed proteins. Ph.D. Thesis, Carnegie Mellon University (1995).
- Song, L., Hennink, E.J., Young, I.T., and Tanke, H.J. Photobleaching kinetics of fluorescein in quantitative fluorescence microscopy. *Biophys. J.* **68:** 2588-2600 (1995).
- Thomas, J., and Webb, W.W. Fluorescence photobleaching recovery: a probe of membrane dynamics. In: *Noninvasive Techniques in Cell Biology*: 129-152 (1990).
- Thompson, N.L., Burghardt, T.P. and Axelrod, D. Measuring surface dynamics of biomolecules by total internal reflection fluorescence with photobleaching recovery or correlation spectroscopy. *Biophys. J.* 33: 435-454 (1981).
- Wells, K.S., Sandison, D.R., Strickler, J., and Webb, W.W. Quantitative fluorescence imaging with laser scanning confocal microscopy. In: The Handbook for Biological Confocal Microscopy. Pawley, J. (ed.), (1989).
- Zimmermann, R.M., Schmidt, C.F., and Gaub, H.E. Absolute quantities and equilibrium kinetics of macromolecular adsorption by fluorescence photobleaching in total internal reflection. *Journal of Colloid and Interface Science* 139: 268-280 (1990).

•

1 }	
i	
)	
'	

